28

BULLETIN Of the International Association of ENGINEERING GEOLOGY
de l'Association Internationale de GÉOLOGIE DE L'INGÉNIEUR No 47 PARIS 1993

COMPUTED SUBSIDENCE OF THE CENTRAL AREA OF SHANGHAI

MODÉLISATION DES TASSEMENTS DANS LA ZONE CENTRALE DE SHANGHAÏ

A. DASSARGUES*, J.P. RADU, R. CHARLIER**, X.L. LI* and Q.F. LI****

Introduction

In the previous papers, all the data have been described and the mathematical concepts of the model explained. Here, the results of the simulations are shown, beginning, as usual, by the calibration procedure and ending with the results of prediction computations.

Calibration of the 3D flow model

The results provided by the model are compared to the measured piezometric maps and to the actual records of the piezometric evolution with time (Dassargues *et al.*) in order to estimate the necessary corrections.

For each run of the numerical model, diagrams showing water pressure versus depth and computed piezometric maps are drawn and a water balance is calculated in order to separate the respective contribution of the lateral boundary fluxes, infiltration from the *phreatic aquifer* (top) and water expelled by compaction.

The global balance of the studied zone can be represented by :

Volume of withdrawal	=	Volume of water expelled from the soil during compaction	+	Volume of water entering by the lateral boundaries	+	Volume of water entering by vertical infiltration (top)

In the first run of the calibration, we have introduced in the model only 8 different materials with different values of K and S_s.

Mainly, the calibration procedure has consisted in changing and adapting the values of the parameters for the different materials.

The successive modifications are shown in Table 1 for run A to run O.

Afterwards, we have determined the value of the parameters in the 14 classes of materials (defined before) on basis of the relatively good results of the run K. The calibration process and its additional modifications are shown in Table 2. It is not very interesting to show here many intermediate results, obtained during calibration, but some comparisons can be made.

For instance, we can compare the diagrams of pressure versus depth at nodes 137 and 209, obtained during run D (Fig. 1 and 2), run K (Fig. 3 and 4) and run C4 (Fig. 5 et 6). We can observe the effects of the increasing contrast between aquitards and aquifers permeabilities, and transient effects in the clayey layers.

Evolution is clearly shown in the computed piezometric maps of 1965 for runs E, G, I (Fig. 7, 8 and 9); the final run C4 has given a computed piezometric map for 1960 very similar to the measured one (Fig. 10).

After the calibration was judged satisfactory until 1965, the model was run until 1975 and then until 1985. Very good results were immediately obtained showing that the detailed calibration, previously completed for the period where big presure variations were involved, was also valid for the next years.

If we consider the integrated water balance of the zone since 1920 until 1985.75, we find :

Total volume	=	Expelled water during consolidation	+	Recharge by infiltration	+	Flow entered by lateral boundaries

* Laboratoires de Géologie de l'Ingénieur, d'Hydrogéologie et de Prospection Géophysique, Université de Liège, Liège, Belgique.
** Département M.S.M., Université de Liège, Liège, Belgique.
* Shanghai Station of Environmental Geology, Shanghai, P.R. China, now at the M.S.M. department, University de Liège, Liège, Belgique.
** Shanghai Station of Environmental Geology, Shanghai, P.R. China.

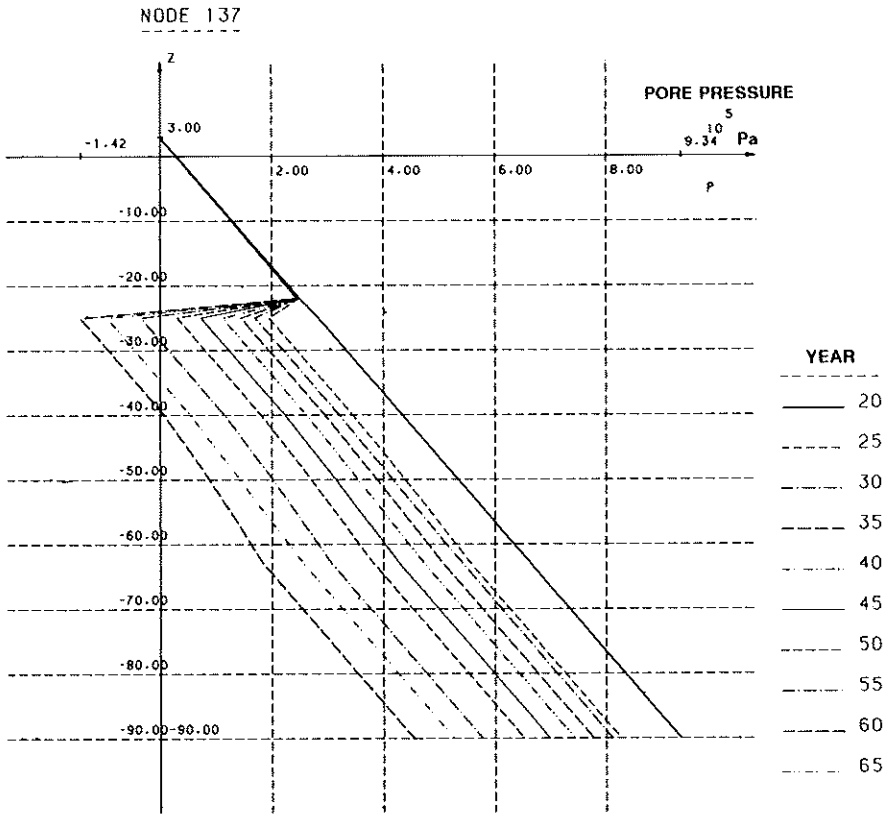

Fig. 1 : Computed pressure diagram at the column 137, at the begining of the calibration (run D)

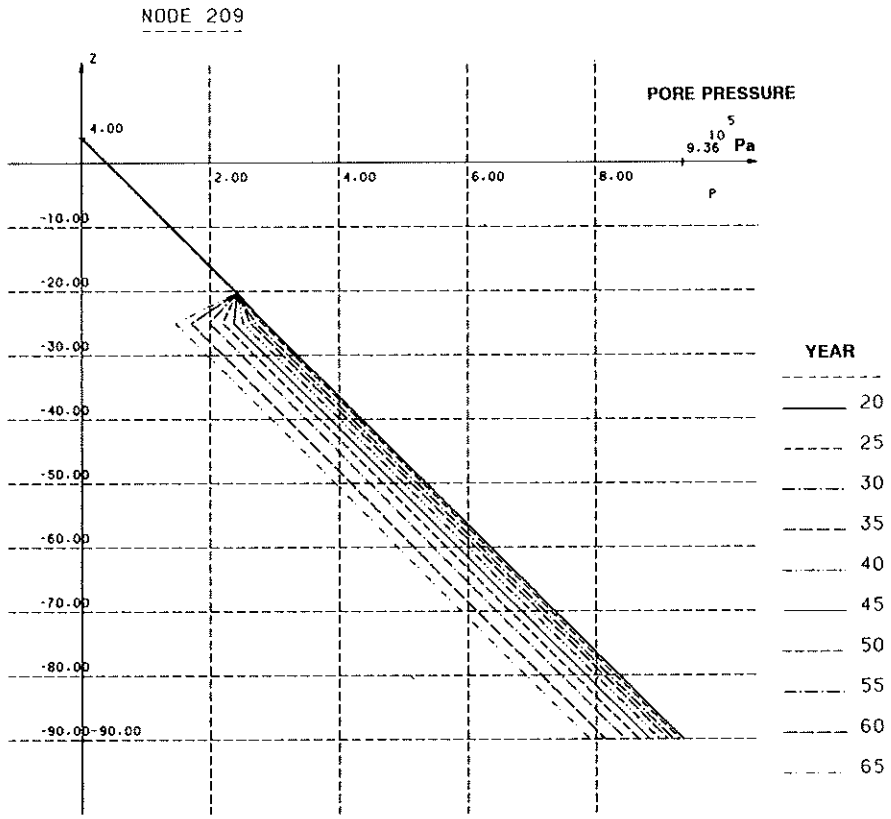

Fig. 2 : Computed pressure diagram at the column 209, at the begining of the calibration (run D)

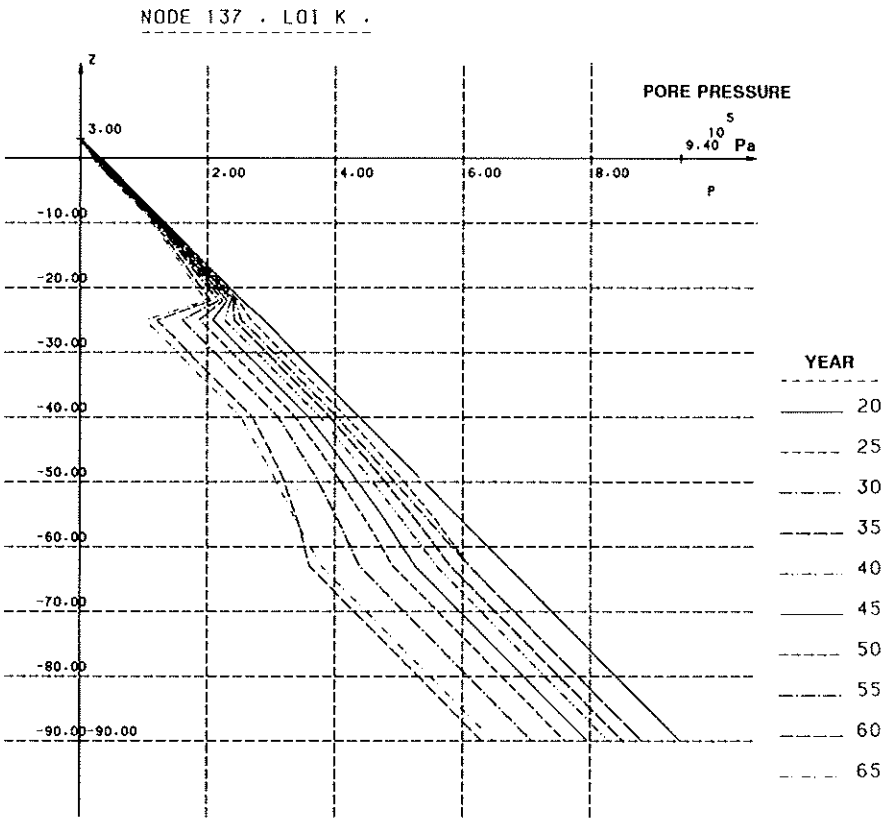

Fig. 3 : Computed pressure diagram at the column 137, run K

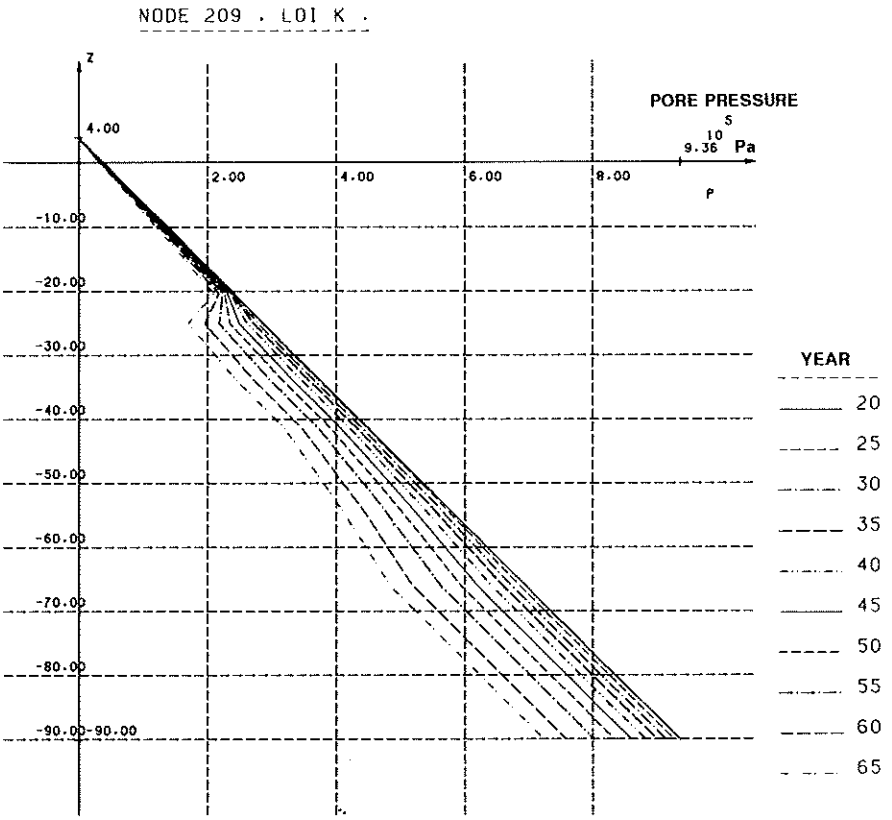

Fig. 4 : Computed pressure diagram at the column 209, run K

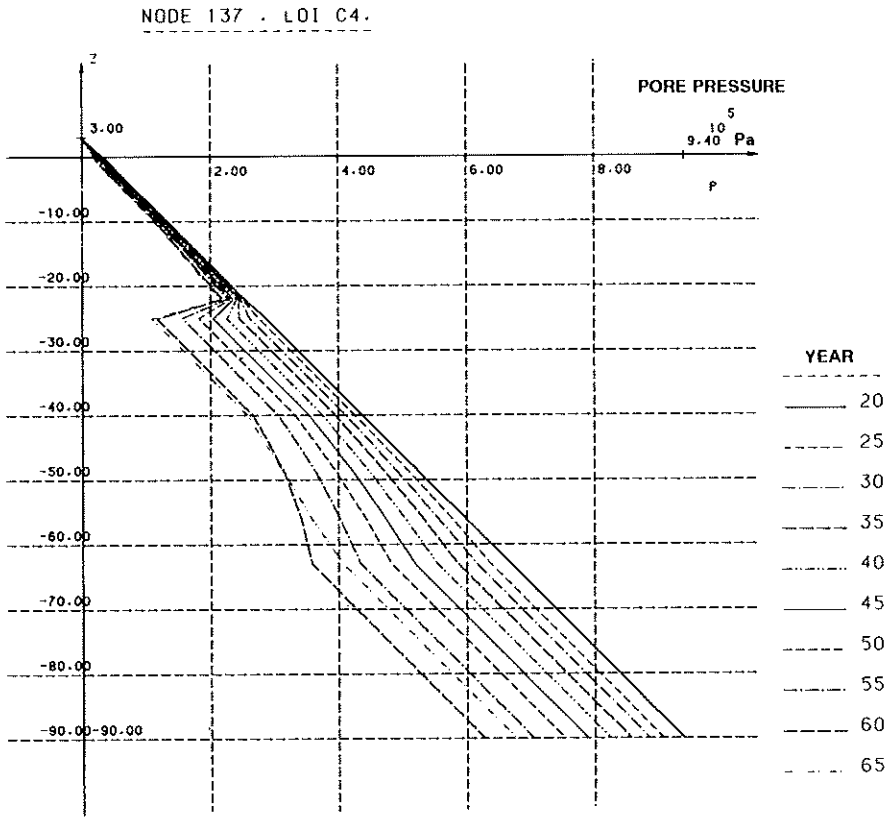

Fig. 5 : Computed pressure diagram at the column 137, run C4

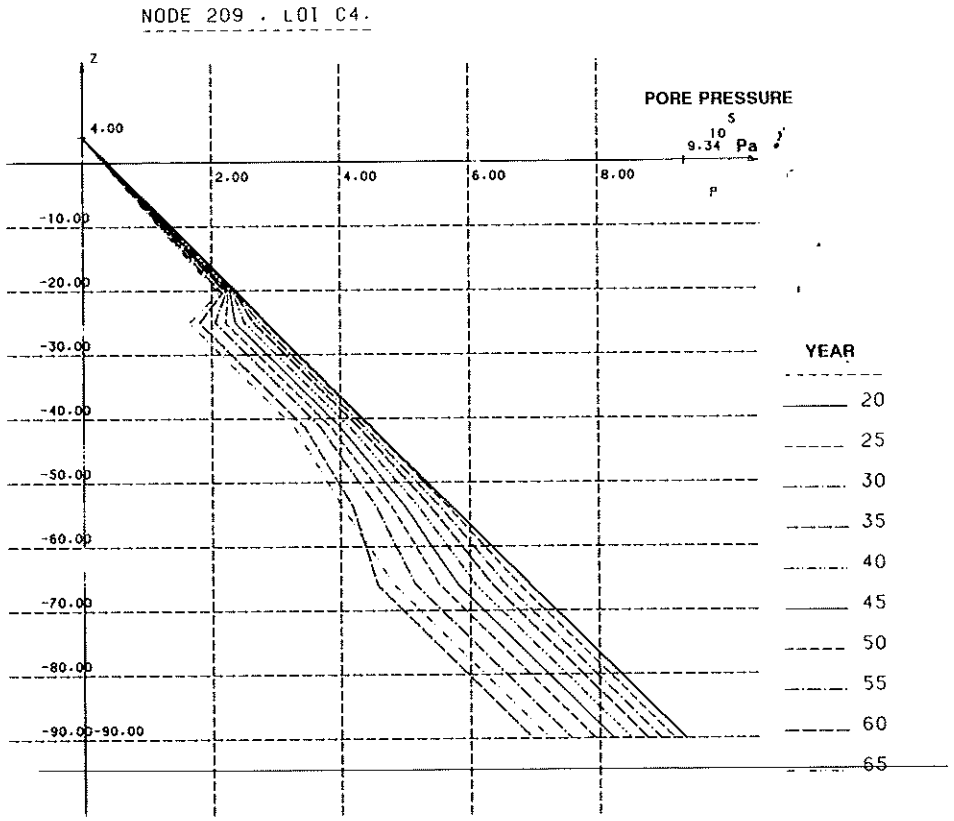

Fig. 6 : Computed pressure diagram at the column 209, run C4

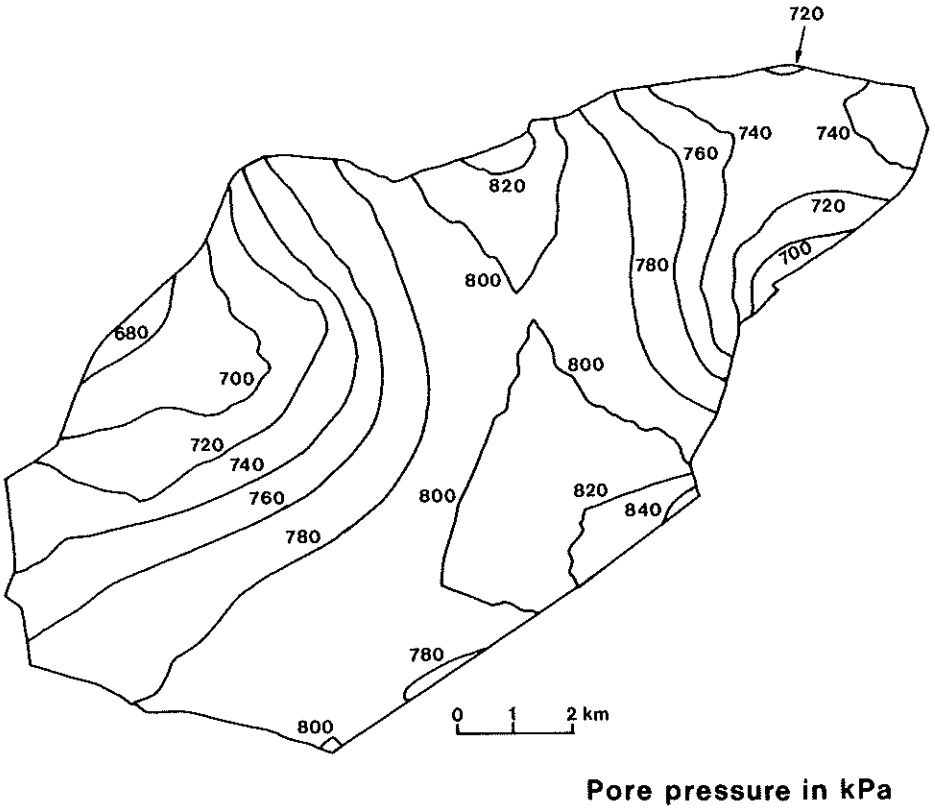

Fig. 7 : Computed piezometric map of 1965, run E

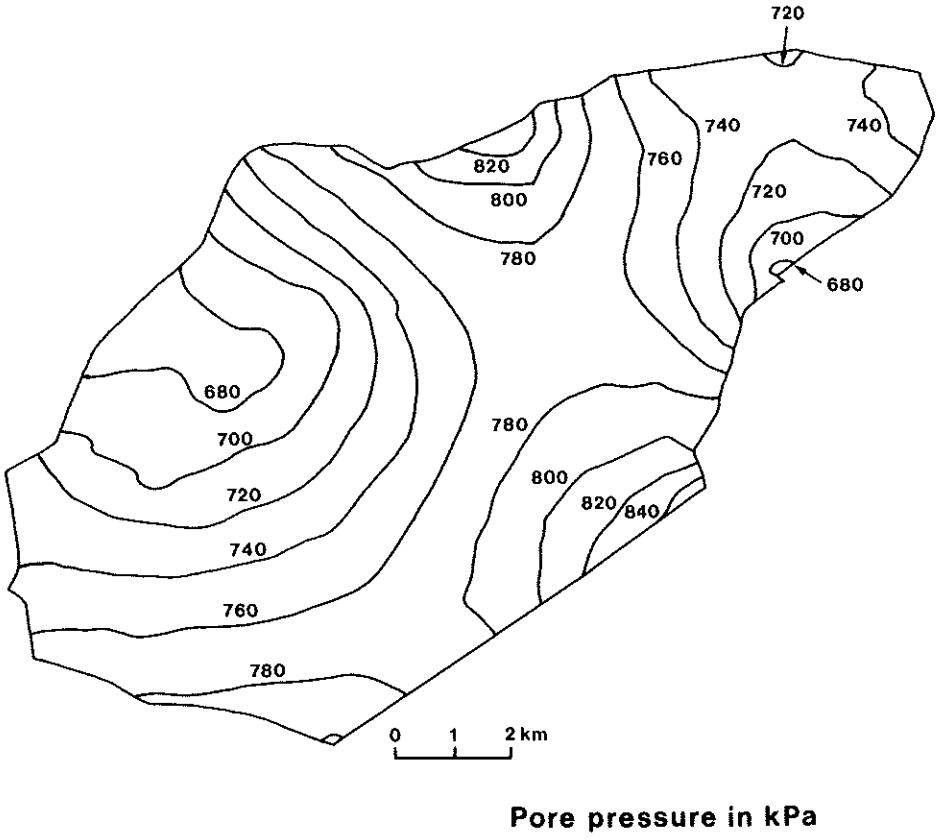

Fig. 8 : Computed piezometric map of 1965, run G

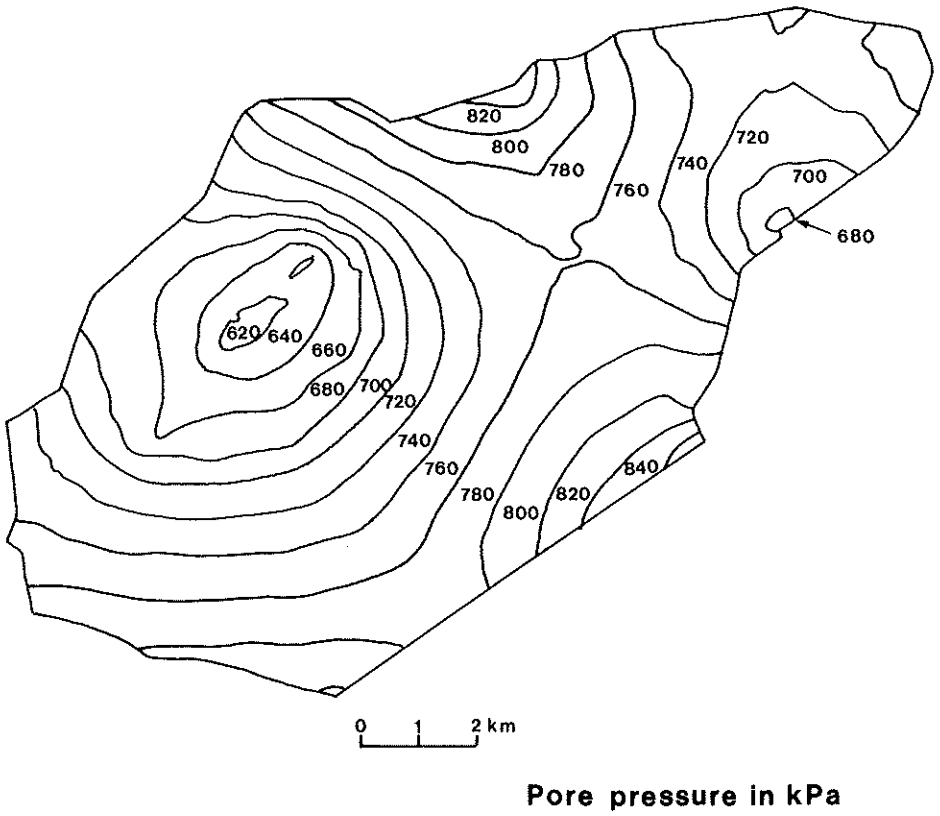

Fig. 9 : Computed piezometric map of 1965, run I

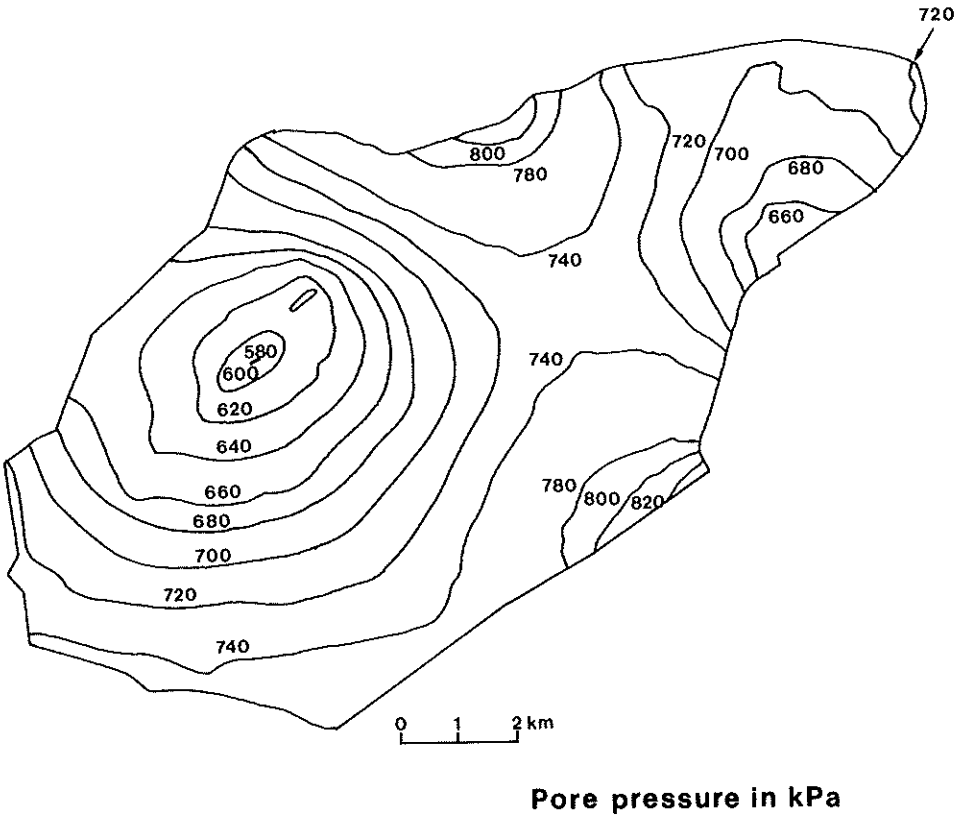

Fig. 10 : Computed piezometric map of 1960, run C4

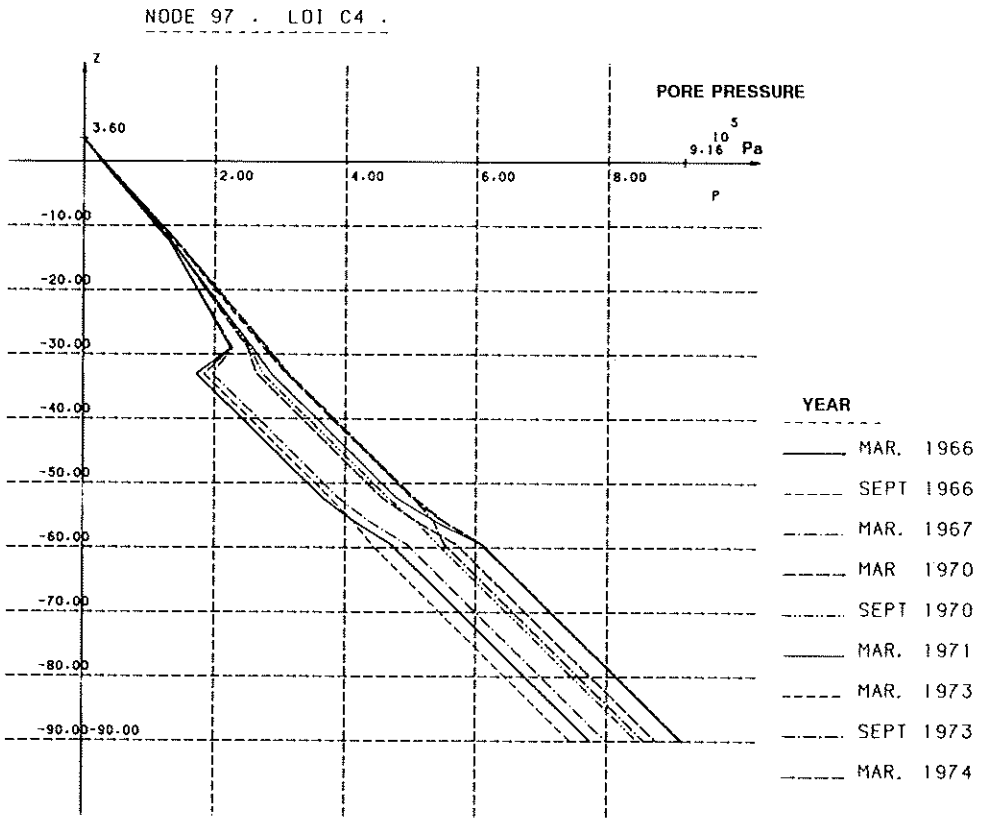

Fig. 11 : Computed pressure diagram at the column 97, from 1966 to 1974

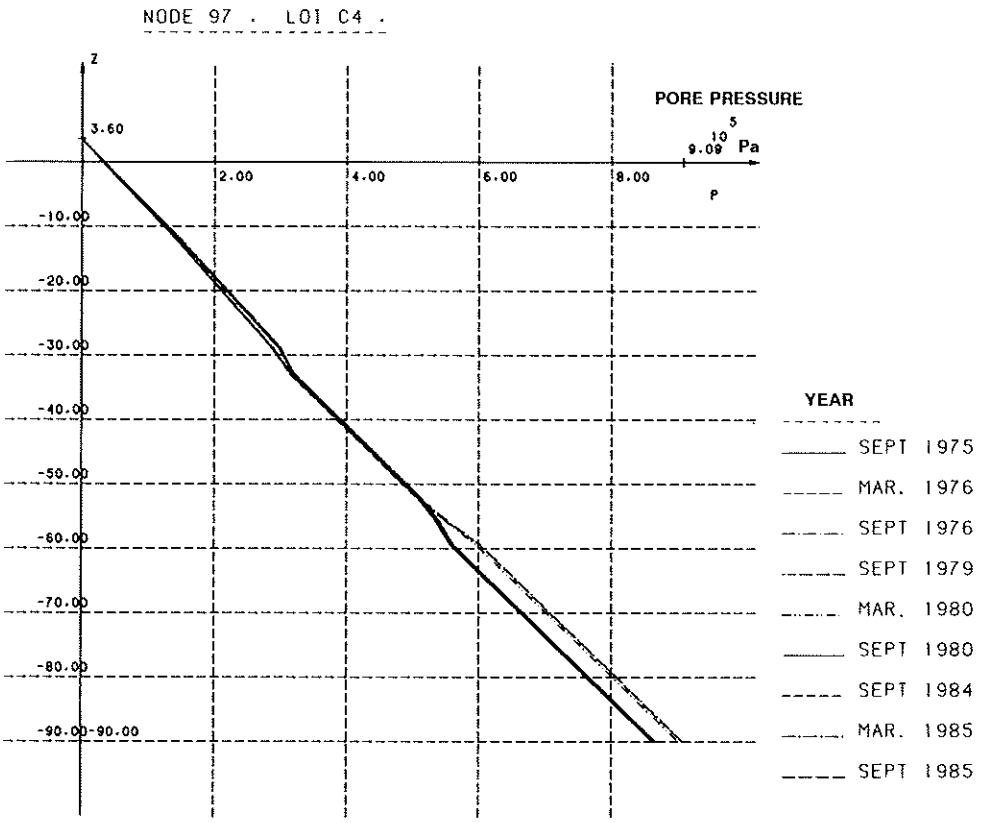

Fig. 12 : Computed pressure diagram at the column 97, from 1975 to 1985

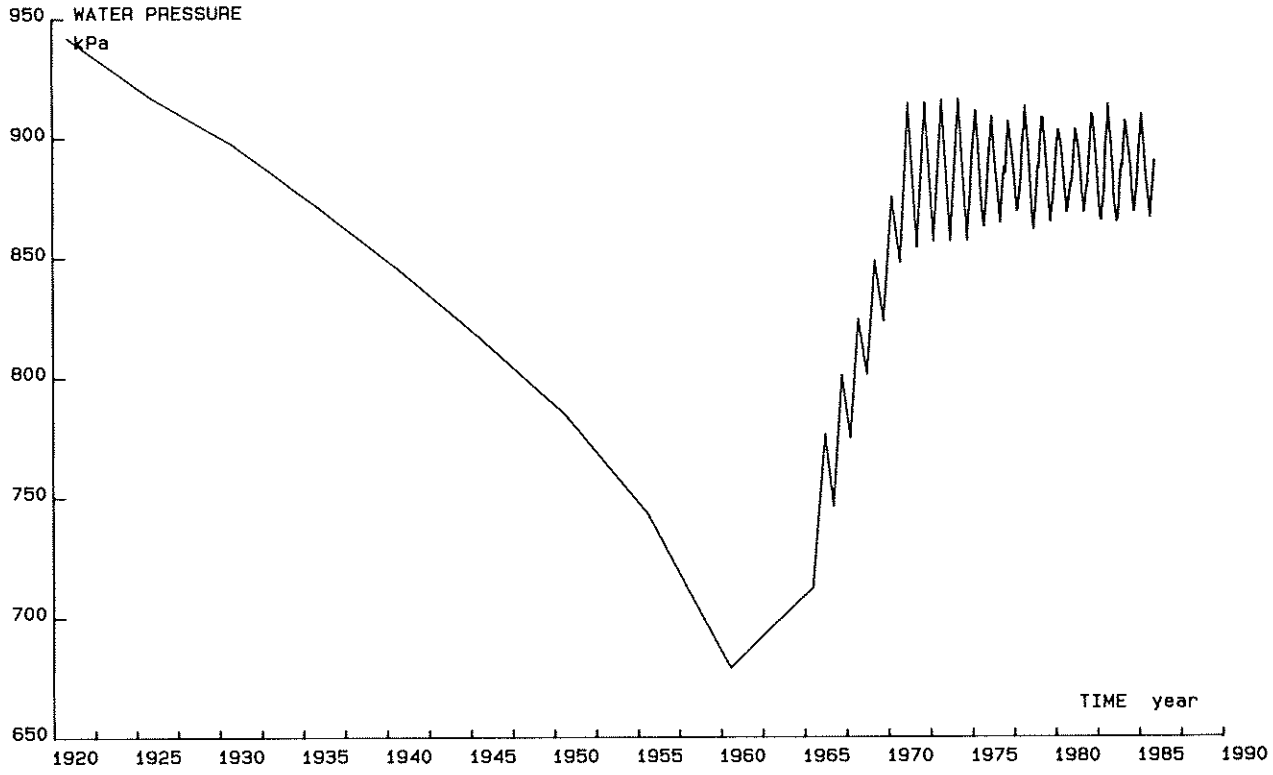

Fig. 13a : Evolution of the computed water pressure (node 160)

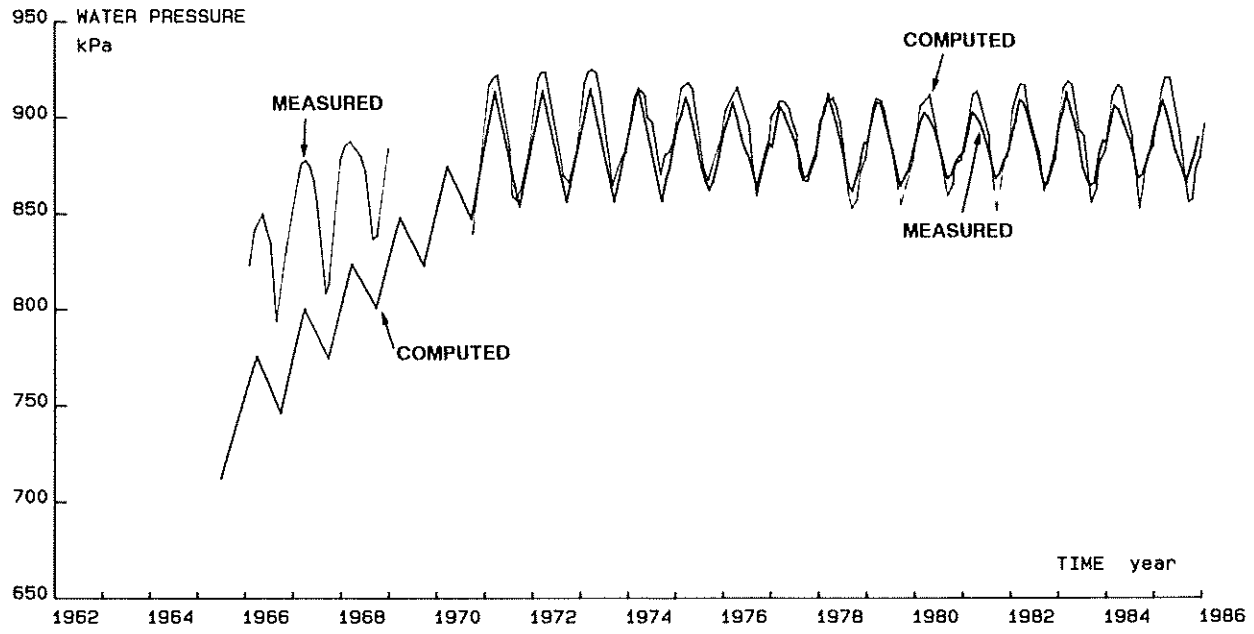

Fig. 13b : Measured and computed pressure below the node 97

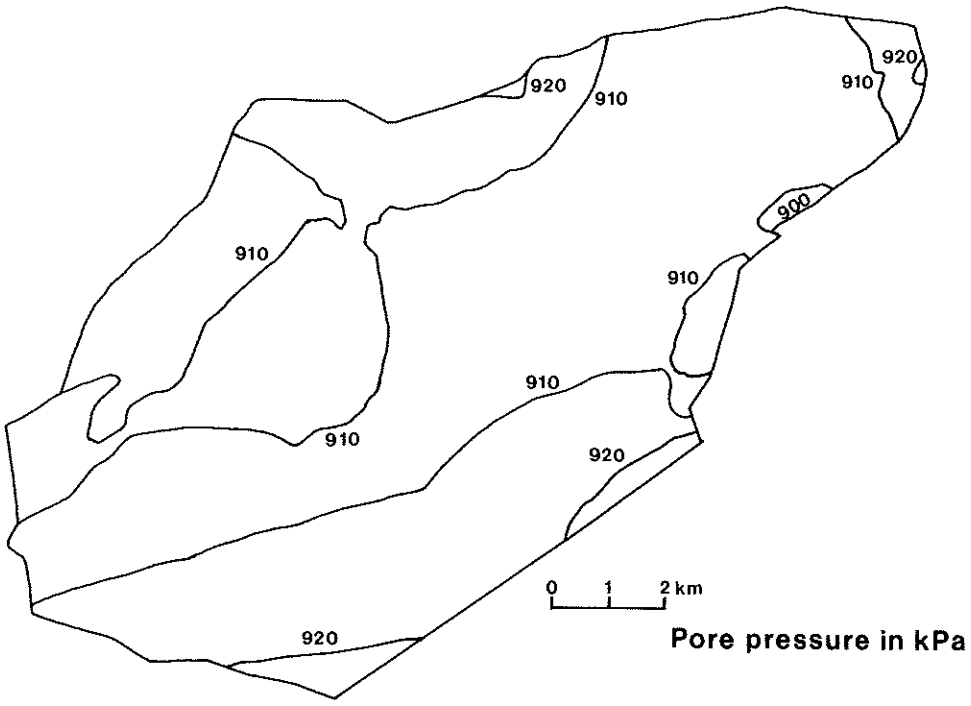

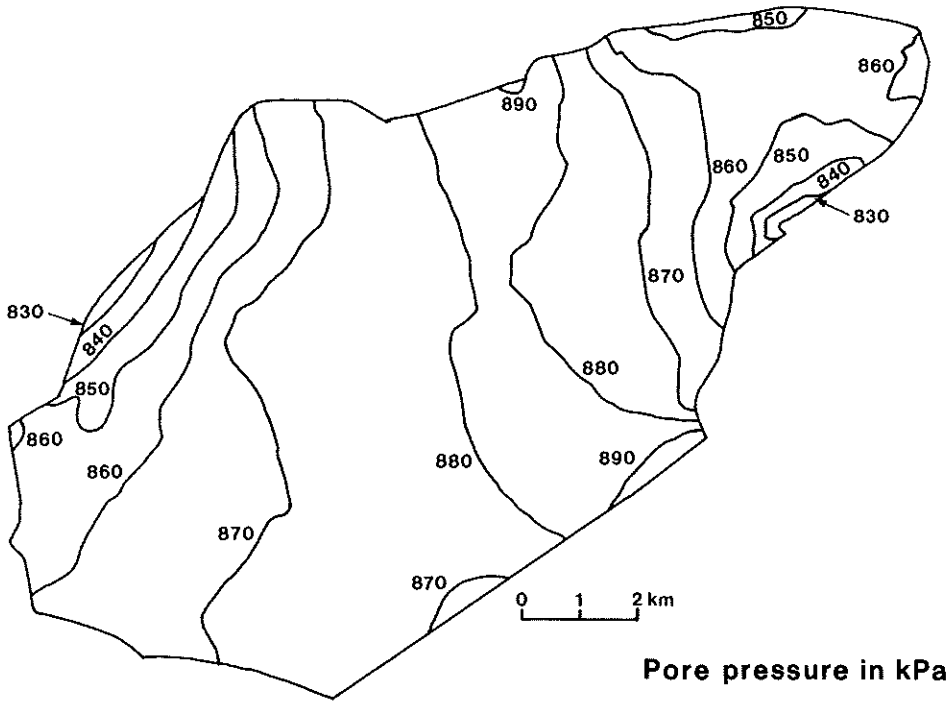

Fig. 14 : Computed pressure maps in March and September 1990

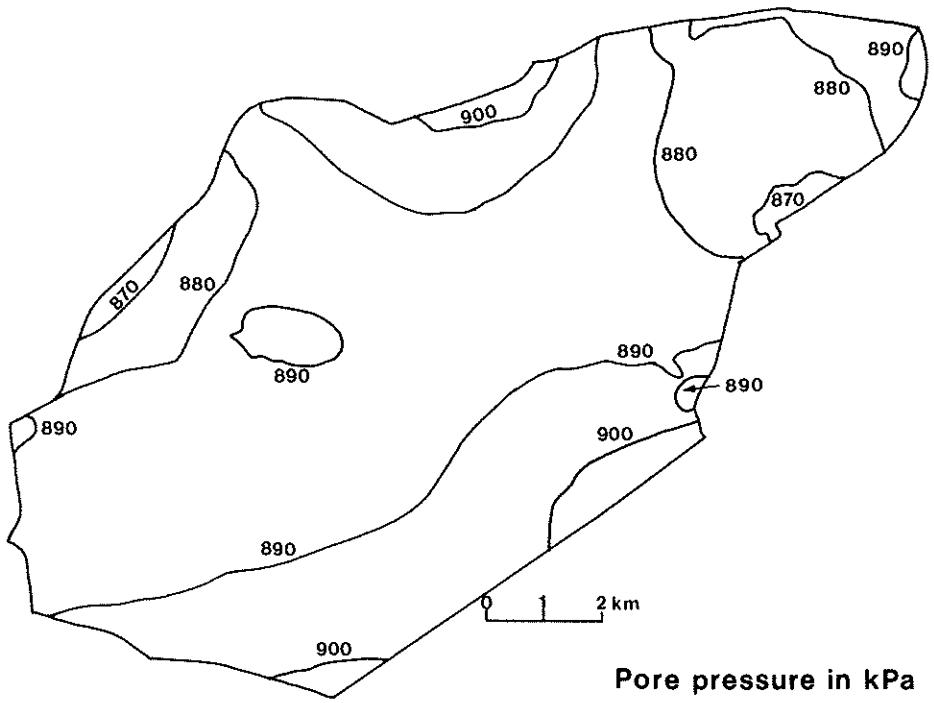

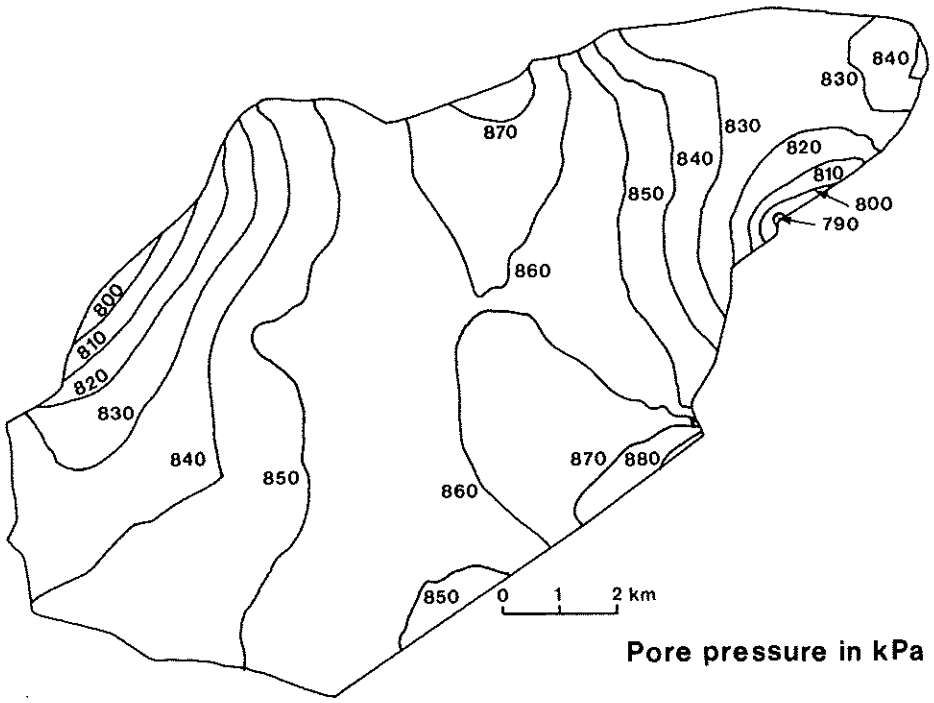

Fig. 15 : Computed pressure maps in March and September 2000

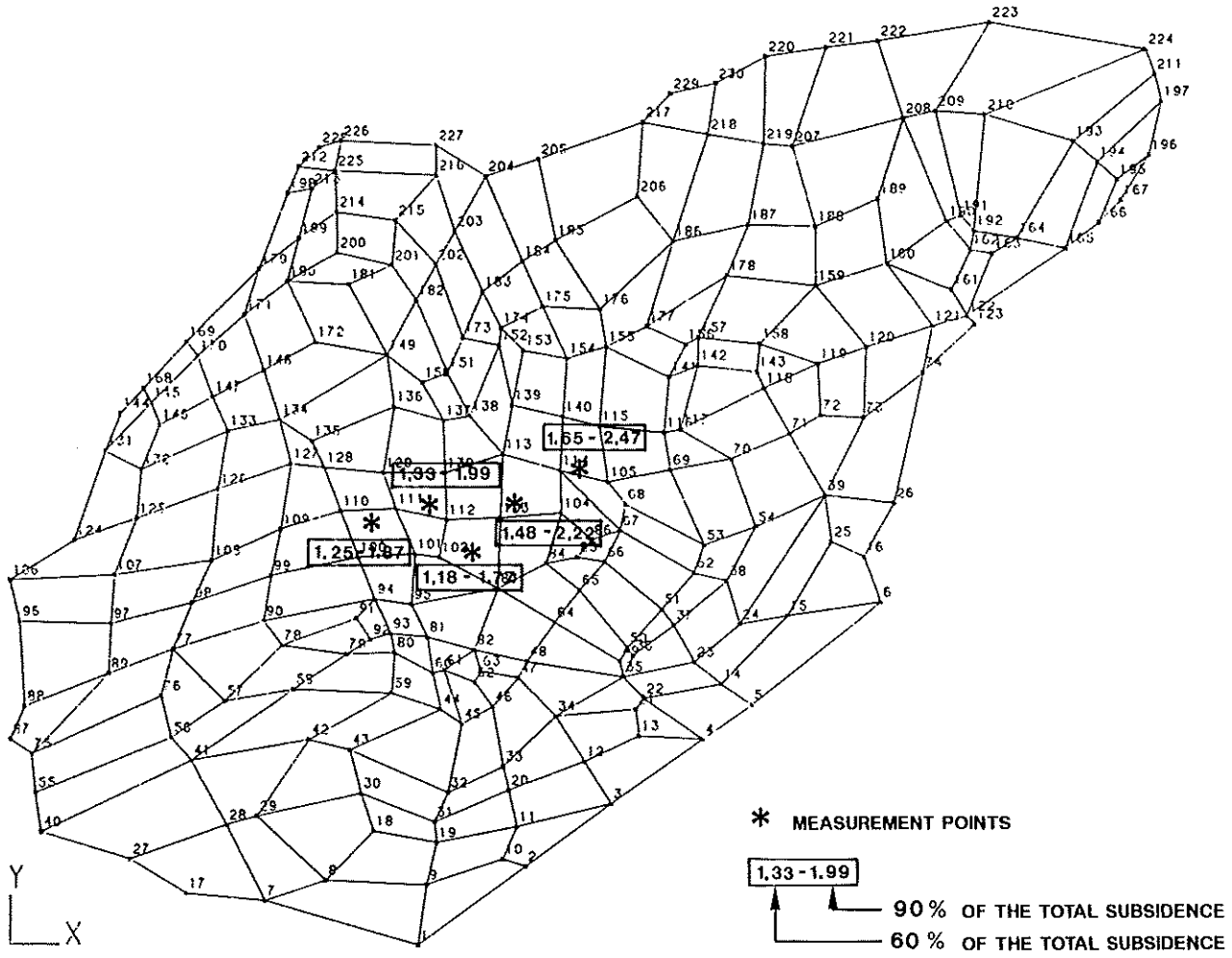

Fig. 16 : Points where total subsidence is measured

$1.17\ 10^9\ m^3$ = Subsidence * $29\ 10^6\ m^2$ + $0.32\ 10^9\ m^3$ + $0.71\ 10^9\ m^3$

The mean subsidence between 1920 and 1985, averaged over the whole modelled area, is about 1.1 m. This value seems to be relatively low and probably is very sensitive to the prescribed boundary conditions.

Pressure versus depth diagrams are given on Figures 11 and 12 for the node 97.

We can check that the water pressures for the month of March are systematically superior to the pressures for September of the same year and we notice the gradual increase of pressure between 1966 and 1974. From 1975 until 1985, only the seasonal variations are still recorded because the mean value of the pressure is approximately constant.

The evolution of the water pressure as a function of time shows a very good agreement between calculated and measured values at different points. The Figure 13 shows an example and one can see that the seasonal variations are well represented.

However during the intensive recharge of the 1965-1975 period, we can remark the poor agreement between calculated and measured values, due to the fact that only bi-annual data of recharge and pumping are available.

In regard to the available data, we can consider the calibration of the 3D model as satisfying.

Sensitivity of the 3D flow model to the boundary conditions

As mentioned previously, the lateral boundaries were first considered impervious (Neuman conditions of zero flux); this assumption is often used when layers are assumed plane and infinite in the lateral direction with respect to their thickness.

In our case, the constraints (pumping and recharge) applied to the groundwater system are located near the lateral boundaries. With a transmissivity value of 2.10^{-2} m^2/sec, the boundary exchanges are greatly influenced by these constraints. But, our study was contractually limited to the central zone of Shanghai (area about 120 km^2).

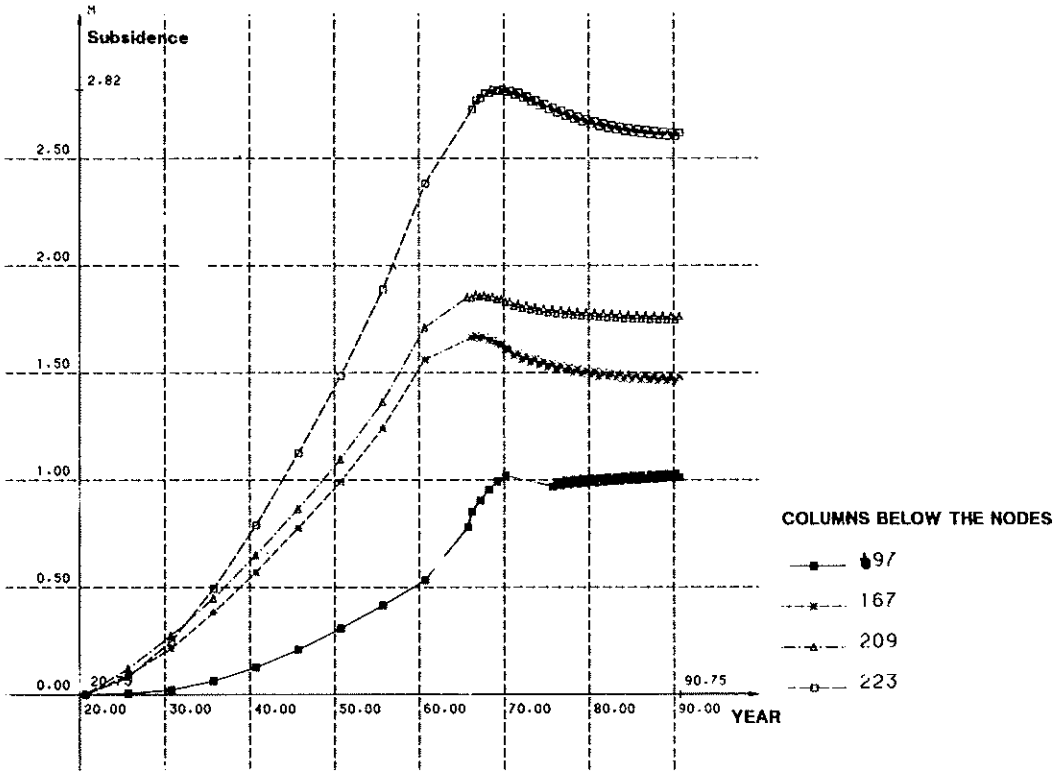

Fig. 17 : Total computed subsidences, columns 197, 167, 209, 223

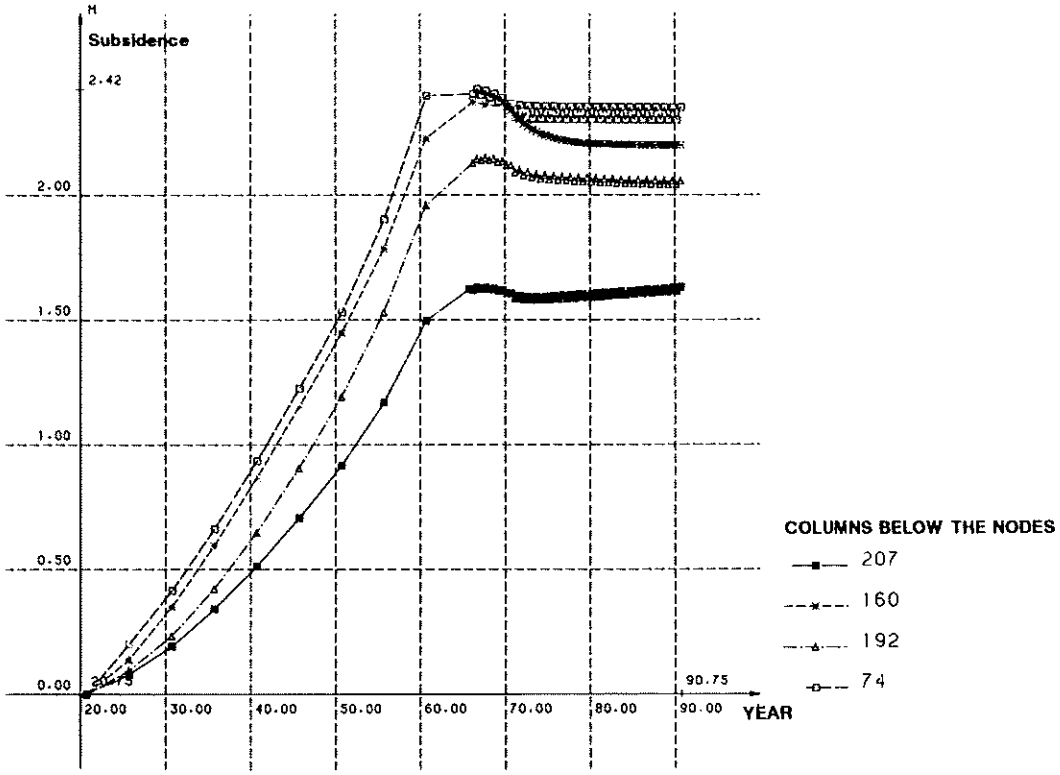

Fig. 18 : Total computed subsidences, columns 207, 160, 192, 74

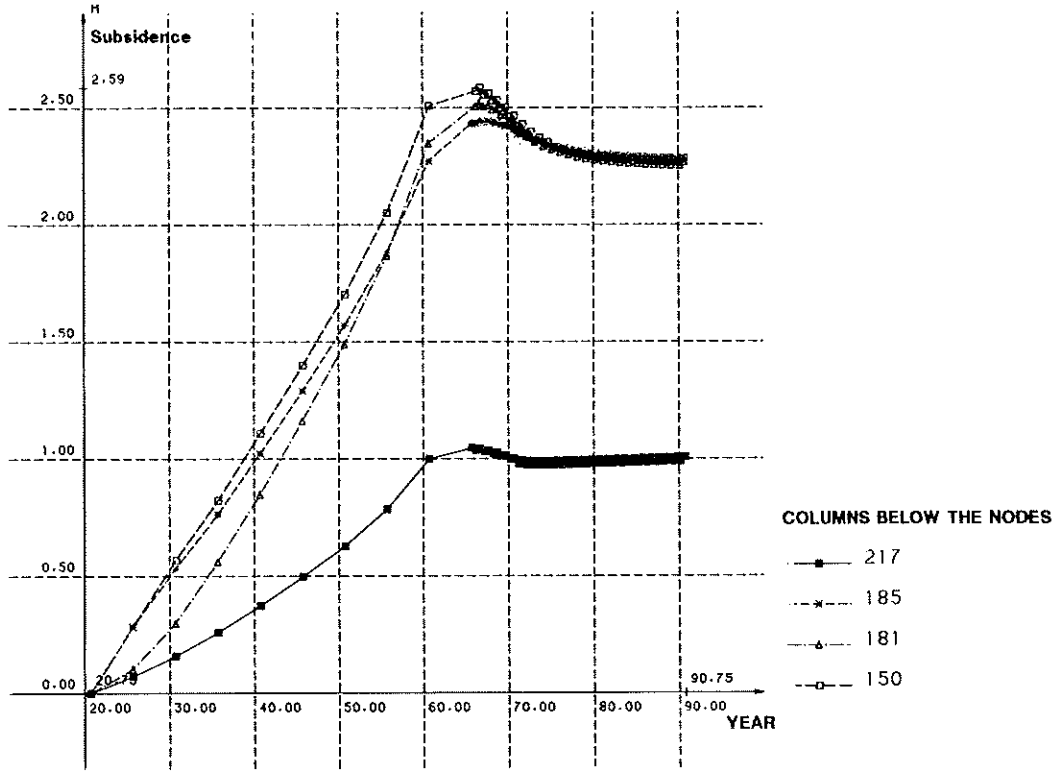

Fig. 19 : Total computed subsidences, columns 217, 185, 181, 150

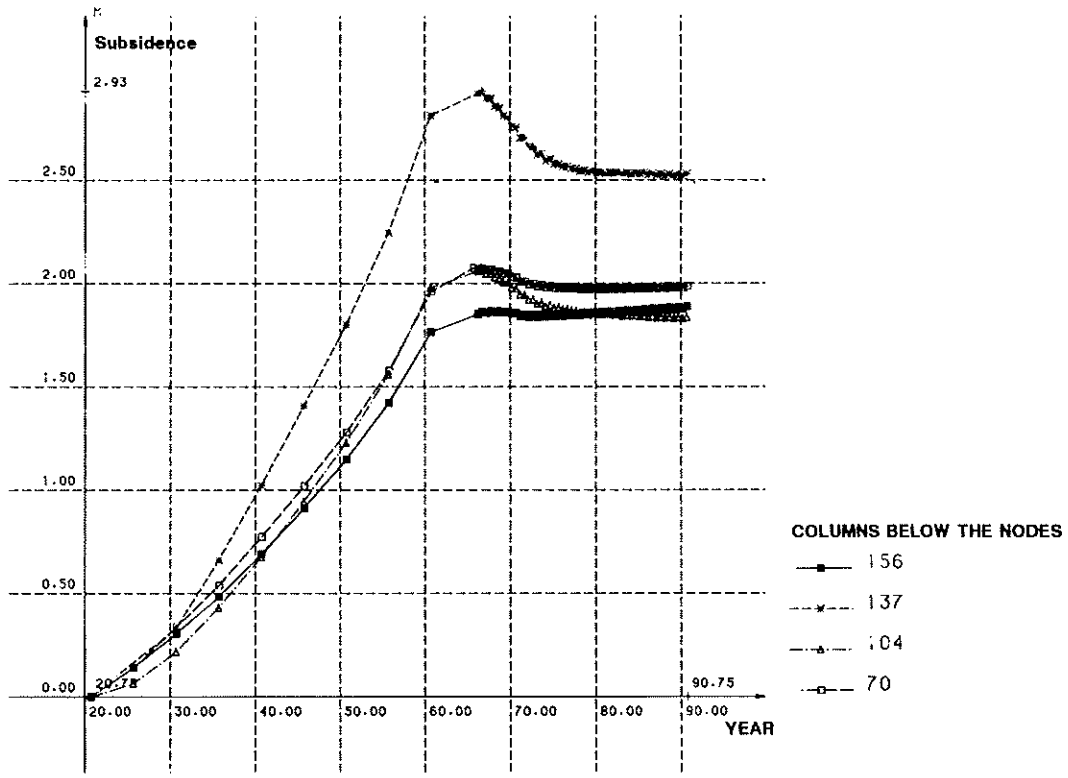

Fig. 20 : Total computed subsidences, columns 156, 137, 104, 70

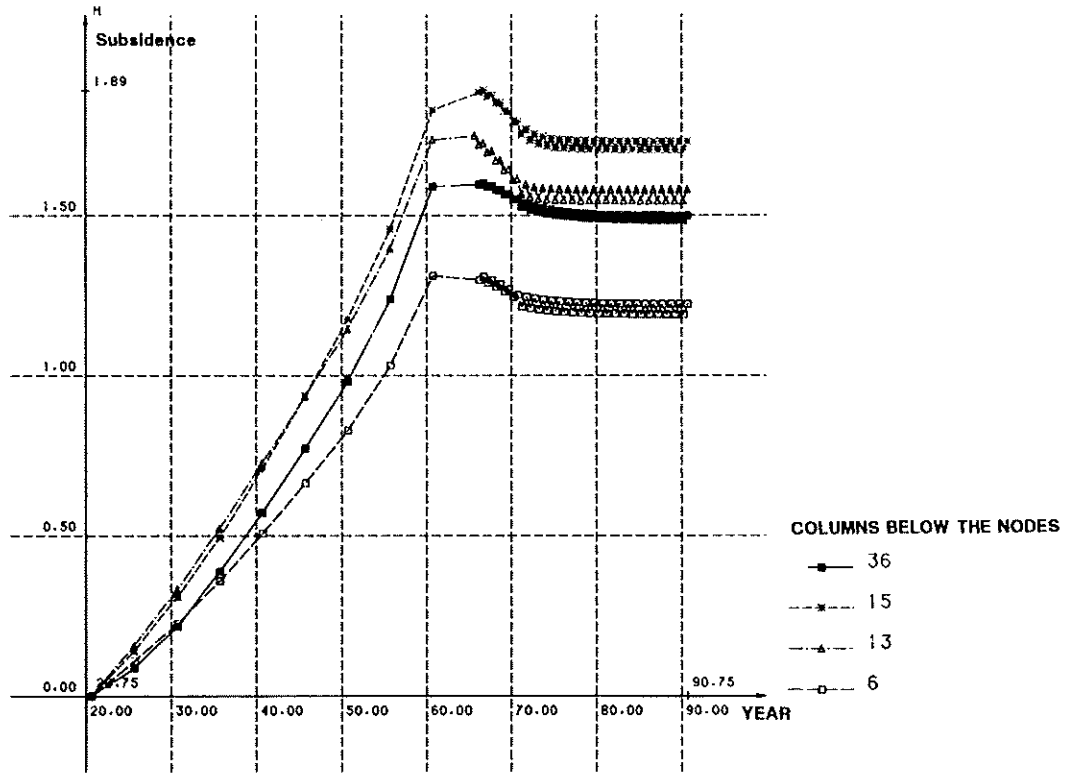

Fig. 21 : Total computed subsidences, columns 36, 15, 13, 6

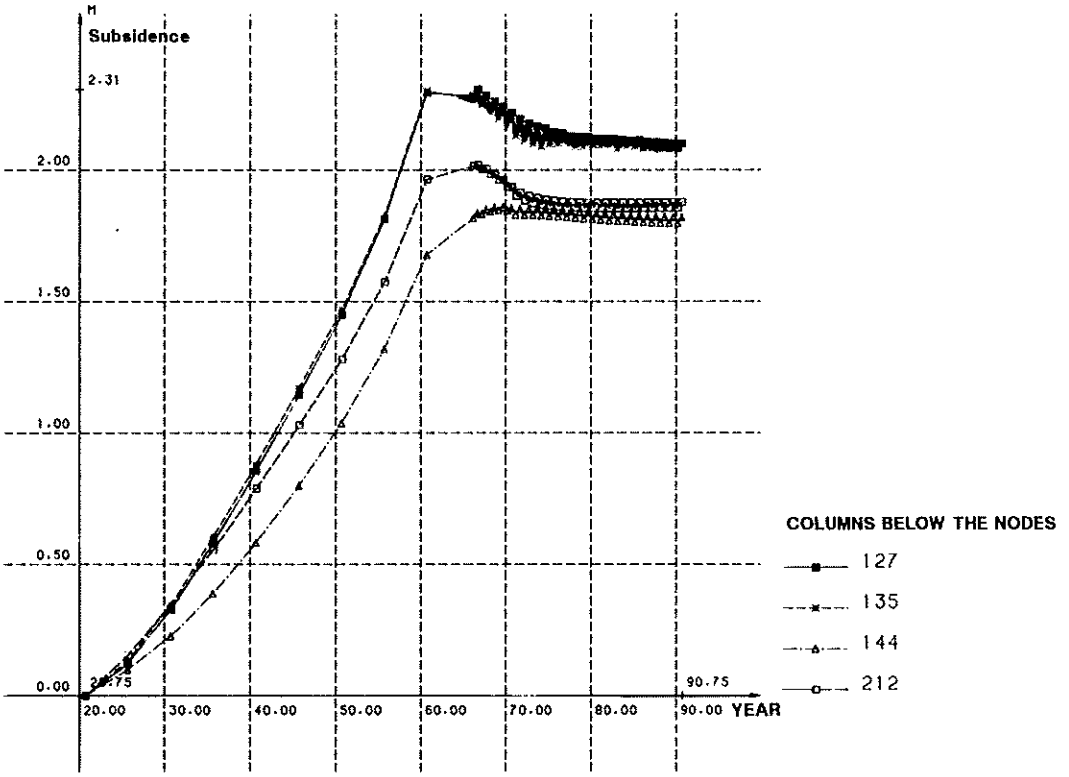

Fig. 22 : Total computed subsidences, columns 127, 135, 144, 212

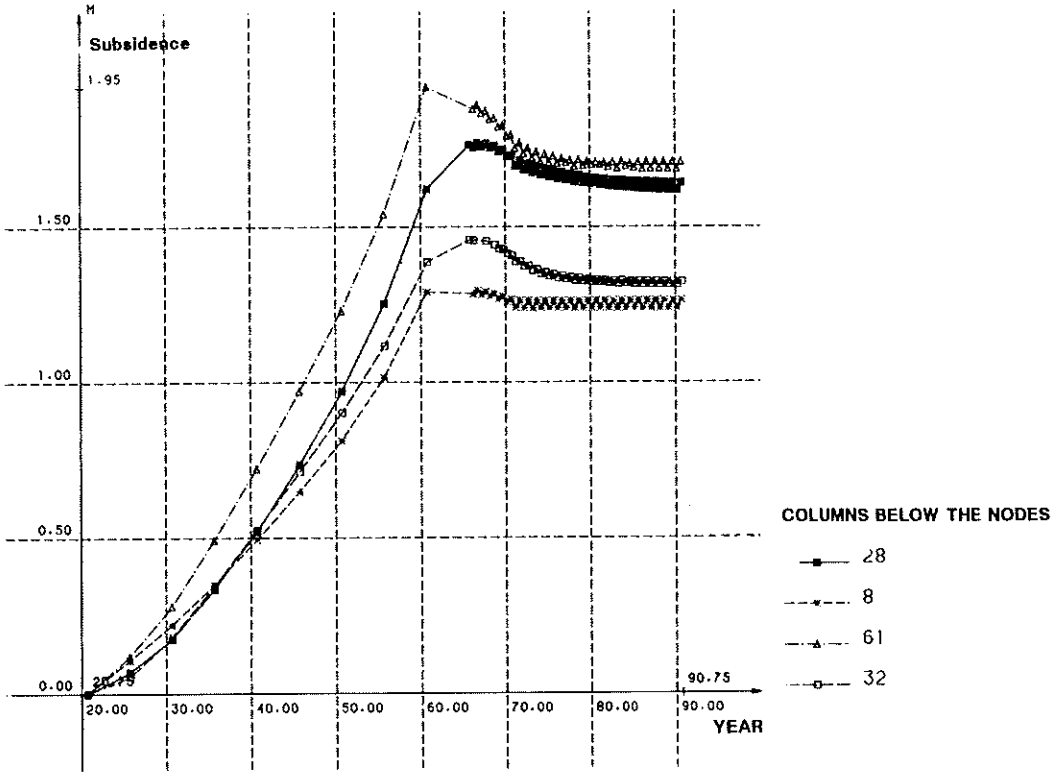

Fig. 23 : Total computed subsidences, columns 28, 8, 61, 32

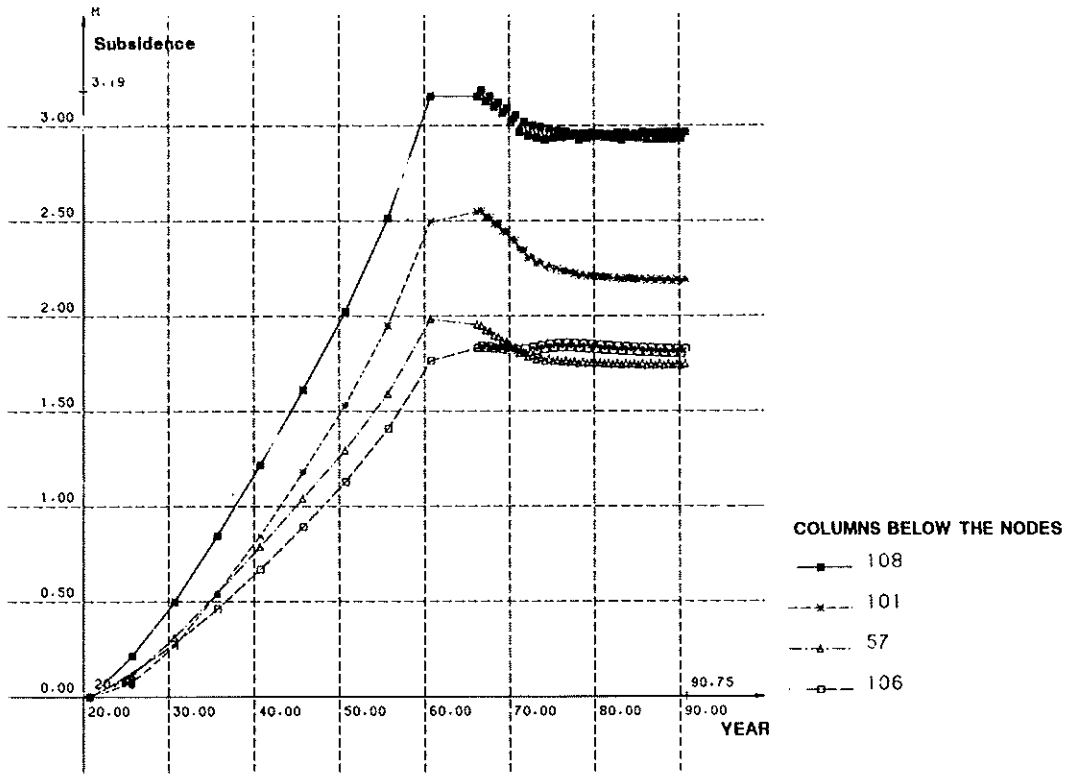

Fig. 24 : Total computed subsidences, columns 108, 101, 57, 106

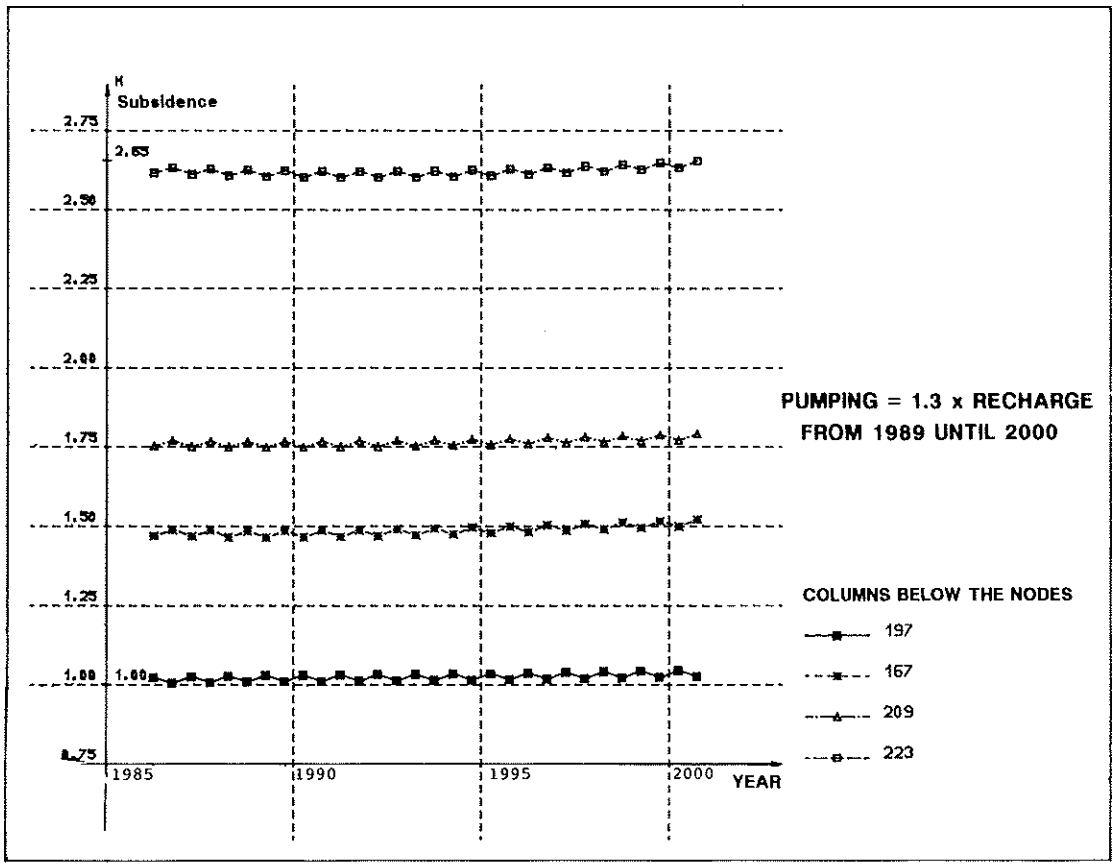

Fig. 25 : Additional computed subsidence, columns 197, 167, 209, 223

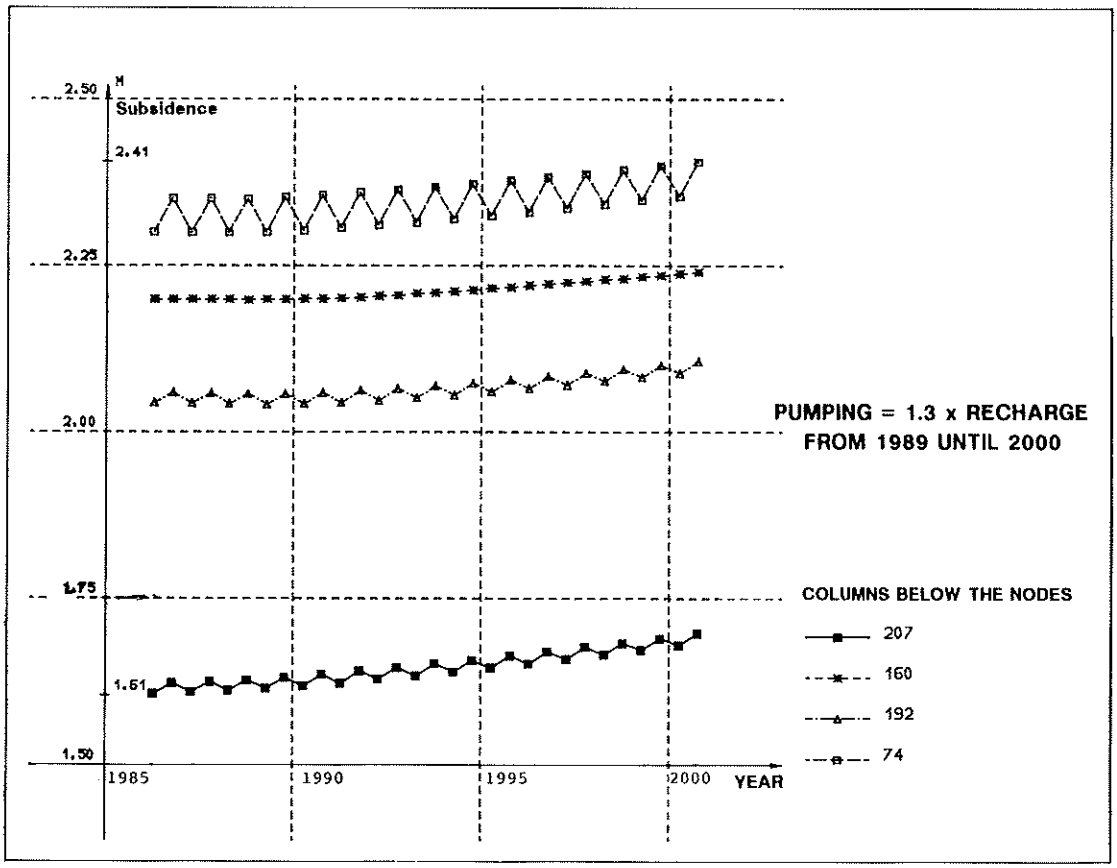

Fig. 26 : Additional computed subsidence, columns 207, 160, 192, 74

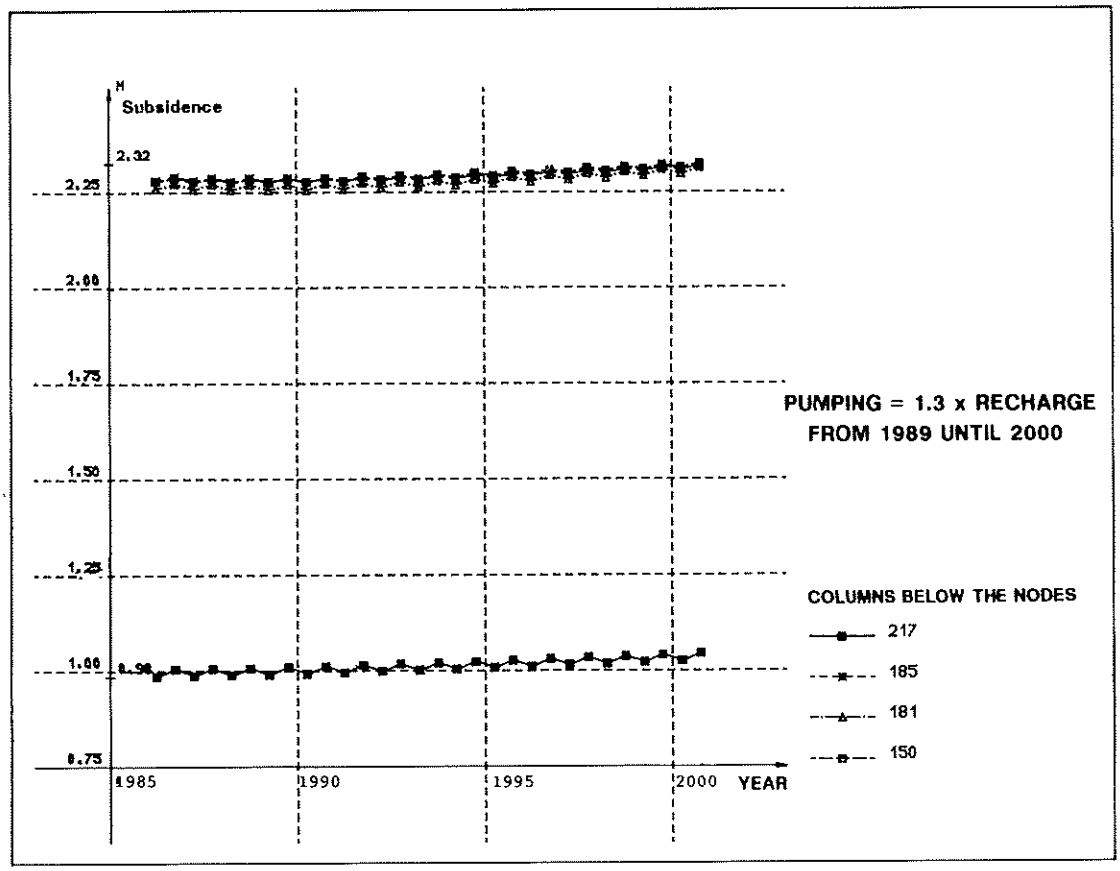

Fig. 27 : Additional computed subsidence, columns 217, 185, 181, 150

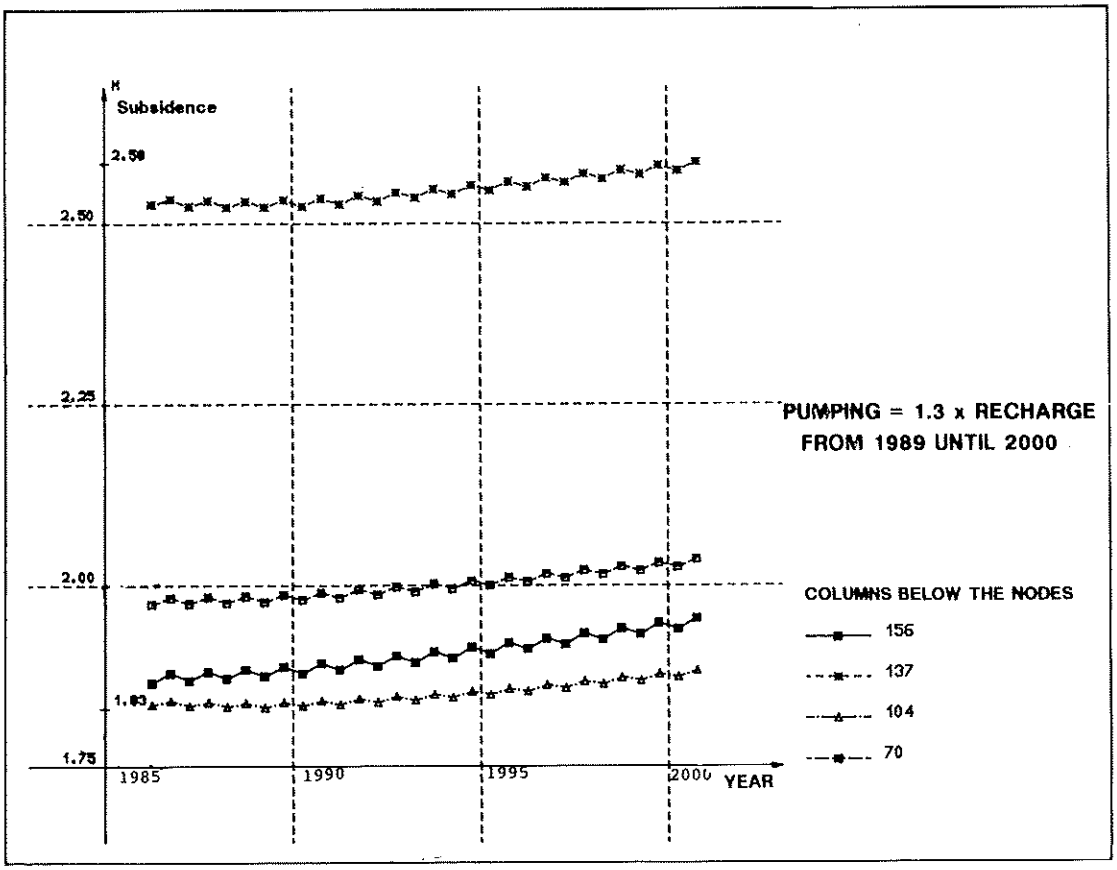

Fig. 28 : Additional computed subsidence, columns 156, 137, 104, 70

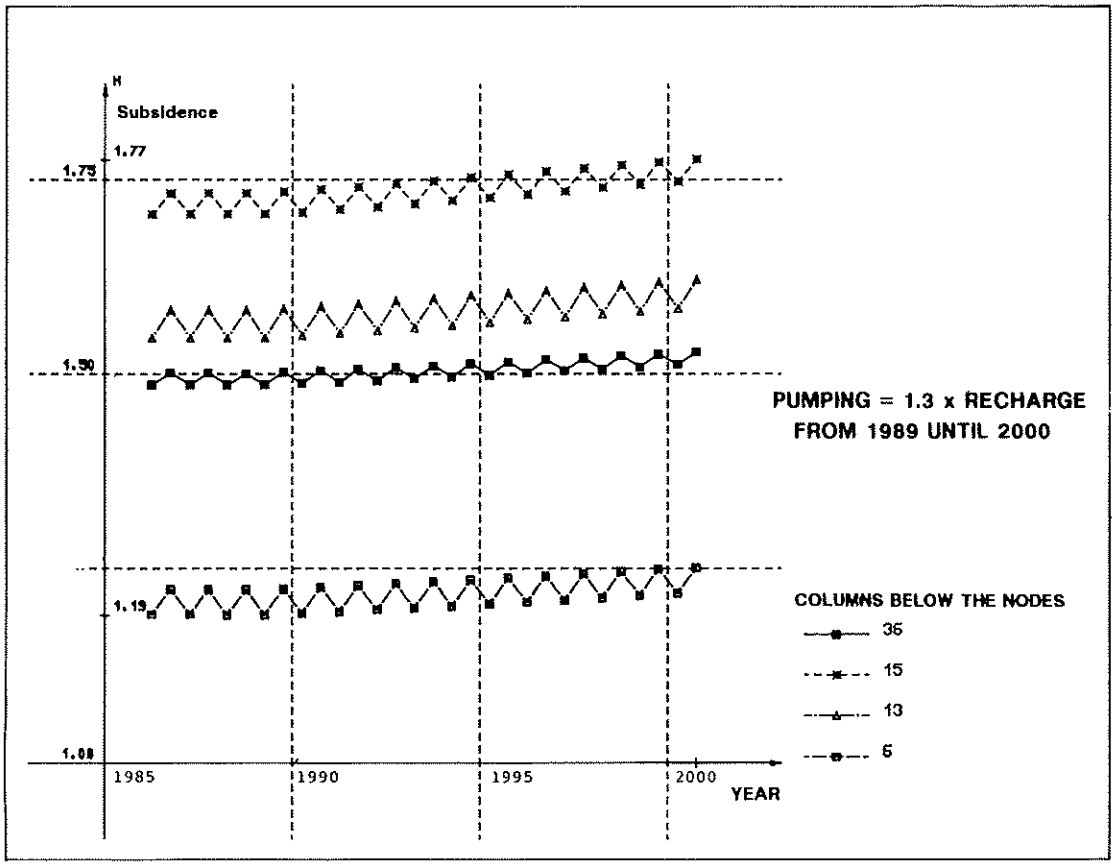

Fig. 29 : Additional computed subsidence, columns 36, 15, 13, 6

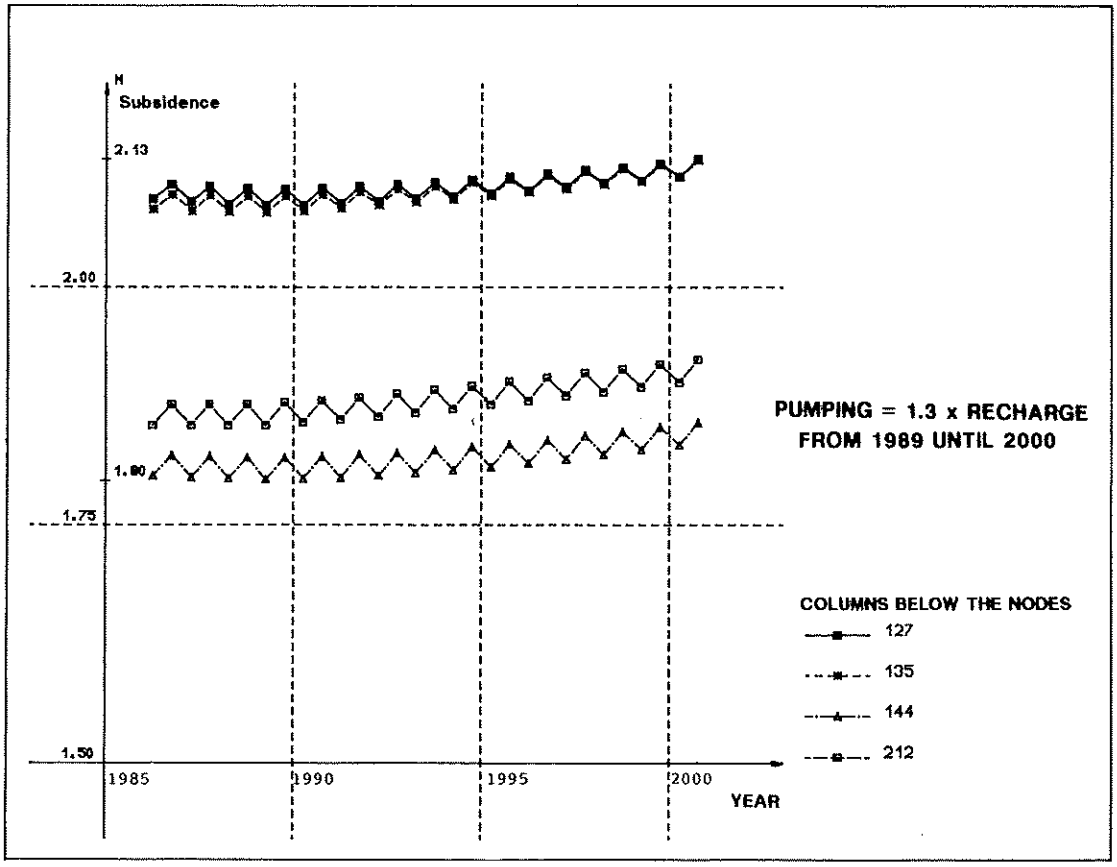

Fig. 30 : Additional computed subsidence, columns 127, 135, 144, 212

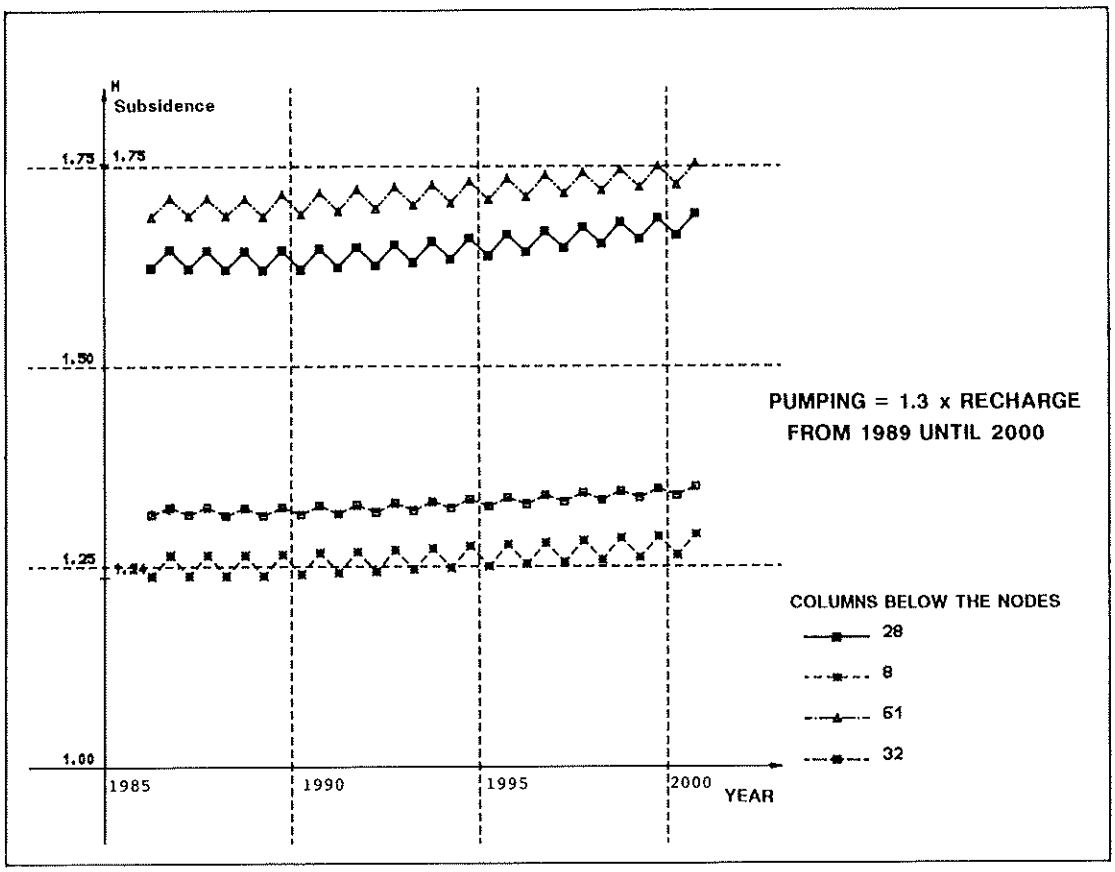

Fig. 31 : Additional computed subsidence, columns 28, 8, 61, 32

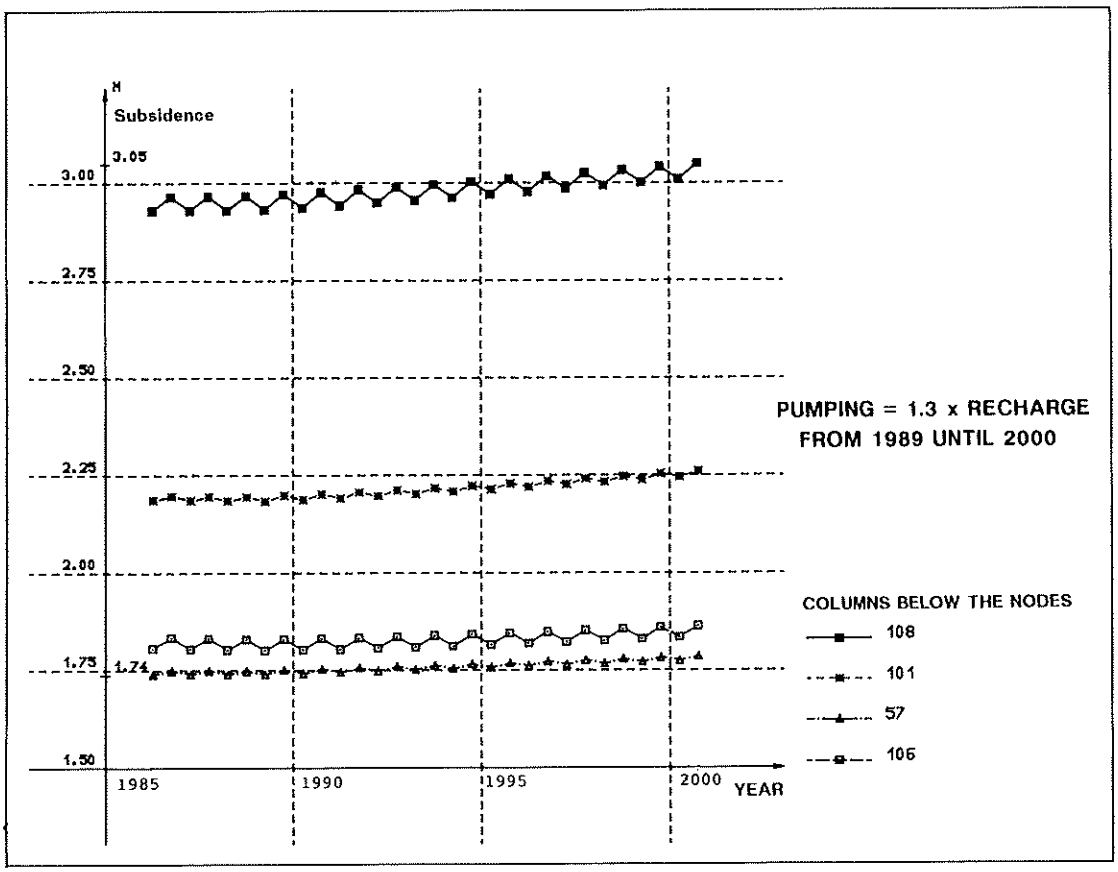

Fig. 32 : Additional computed subsidence, columns 108, 101, 57, 106

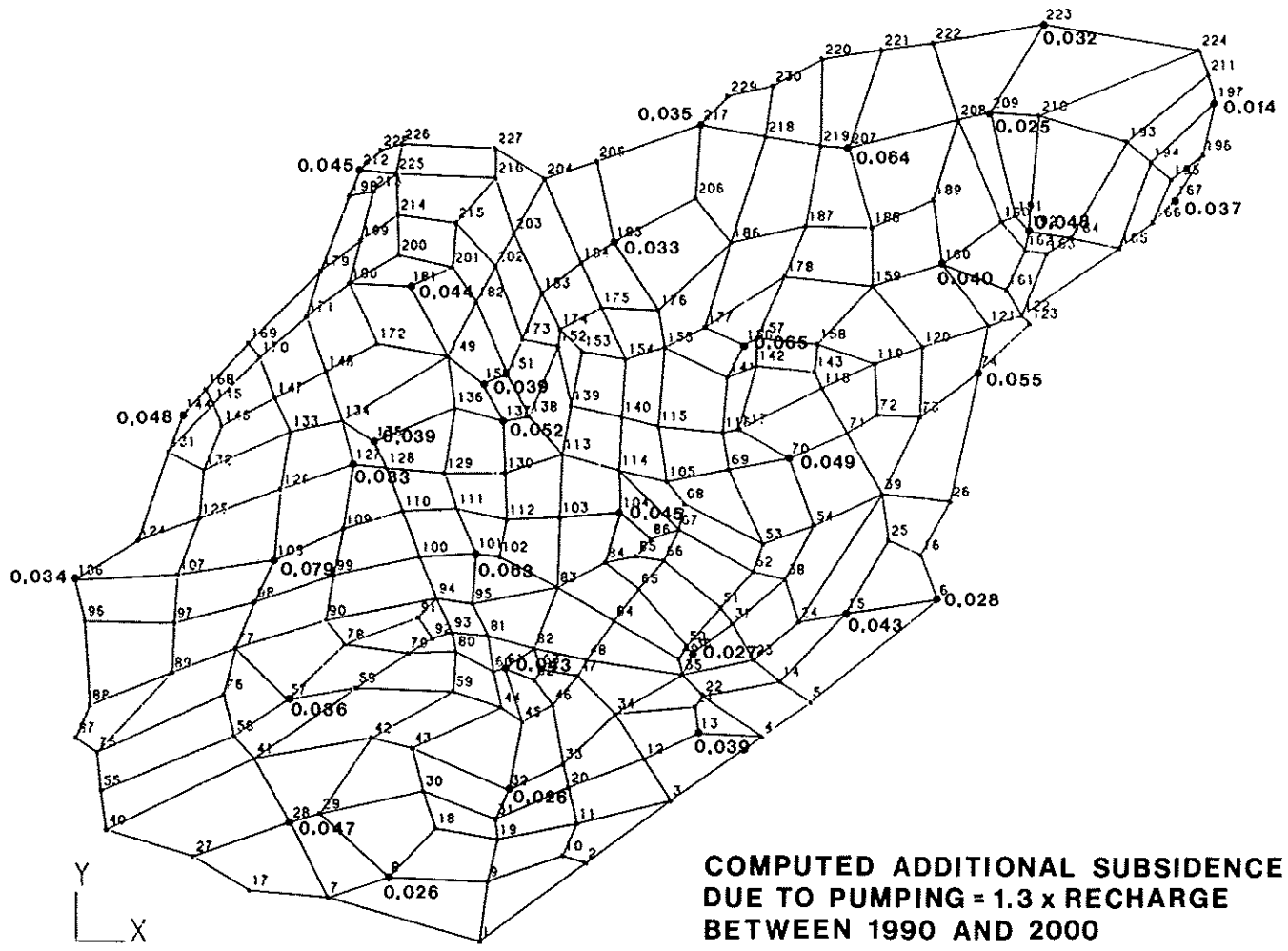

Fig. 33 : Map showing the computed additional subsidence

With the same discretization as before, time varying prescribed pressures have been imposed on the lateral boundaries. They have been determined not only from the measured pressures but also in function of the pumping rate in the modelled zone, using a multiplication coefficient (Dassargues *et al.*). During the seasonal variations, this coefficient takes the value of + 0.04 (pumping) and – 0.04 (recharge).

In fact, when introducing this coefficient, we have to admit that we impose part of the solution and this will put forward some problems for prediction computations.

According to the information of the Shanghai Geological Bureau, pumping and even maybe recharge occurred very often in the neigbouring zones of the model since 1965. But neither quantitative nor qualitative information is available concerning this problem. So that it is very difficult to estimate the lateral fluxes of the model after 1965.

In the future, it will be convenient to impose prescribed pressures on lateral boundaries located further away from the main stressed zone or convective boundary conditions as it has been mentioned above (Charlier *et al.*).

Simulations for the future with the 3D flow model

Keeping in mind the above remarks about the sensitivity of the model to the boundary conditions, a simulation is completed with pumping = 1.3 * recharge* from 1988.75 until the year 2000.

The multiplication coefficient of the boundary is empirically adapted to obtain + 0.0419 (pumping) and – 0.04 (recharge).

The maps of computed water pressure, in March and September, are shown for 1990 (Fig. 14) and 2000 (Fig. 15).

Calibration of the compaction model

The non-linearity of the permeability coefficient is introduced by the Nishida relation (Dassargues *et al.*). The non-linearity of the specific storage coefficient and the flow-compaction coupling are introduced by the constitutive law $f^v = \dot{e}$ (Dassargues *et al.*) and Charlier *et al.*).

* The year 1978 has been taken as reference.

Table 1 : Successive modifications of the parameters.

	A	B	C	D	E	F	G	H	I	J	K	L	M	N	O
mat 1 K	$1\ 10^{-9}$	$1\ 10^{-7}$	-	-	-	-	-	-	-	-	$1\ 10^{-8}$	$1\ 10^{-9}$	-	-	-
S_{sp}	$1.69\ 10^{-7}$	-	-	-	-	-	-	-	-	-	$1.69\ 10^{-7}$	-	-	-	-
mat 2 K	$1\ 10^{-5}$	$1\ 10^{-6}$	$1\ 10^{-5}$	-	-	-	-	-	-	-	$1\ 10^{-5}$	-	-	-	-
S_{sp}	$0.22\ 10^{-7}$	-	-	-	-	-	-	-	-	-	$0.22\ 10^{-7}$	-	-	-	-
mat 3 K	$1\ 10^{-8}$	$1\ 10^{-7}$	-	-	-	$1\ 10^{-8}$	-	-	-	-	$1\ 10^{-8}$	-	-	$5\ 10^{-9}$	-
S_{sp}	$4\ 10^{-7}$	-	-	-	-	-	-	-	-	-	$4\ 10^{-7}$	-	-	-	-
mat 4 K	$1\ 10^{-9}$	$1\ 10^{-7}$	-	$1\ 10^{-9}$	-	-	-	-	-	-	$1\ 10^{-9}$	-	$1\ 10^{-10}$	$1\ 10^{-9}$	$5\ 10^{-10}$
S_{sp}	$0.1\ 10^{-7}$	-	-	-	-	-	-	-	-	-	$0.1\ 10^{-7}$	-	-	-	-
mat 5 K	$1\ 10^{-7}$	$1\ 10^{-7}$	-	-	-	-	-	$1\ 10^{-8}$	-	-	$1\ 10^{-8}$	-	-	-	-
S_{sp}	$3.18\ 10^{-7}$	-	-	-	-	-	-	-	-	-	$3.18\ 10^{-7}$	-	-	-	-
mat 6 K	$1\ 10^{-8}$	$1\ 10^{-7}$	-	-	-	-	-	-	-	$1\ 10^{-8}$	$1\ 10^{-8}$	-	-	-	-
S_{sp}	$4.11\ 10^{-7}$	-	-	-	-	-	-	-	-	-	$4.11\ 10^{-7}$	-	-	-	-
mat 7 K	$1\ 10^{-4}$	-	-	-	-	-	-	-	-	-	$1\ 10^{-4}$	-	-	-	-
S_{sp}	$1\ 10^{-9}$	$0.2\ 10^{-9}$	-	-	-	-	-	-	-	-	$0.2\ 10^{-9}$	-	-	-	-
mat 8 K	$1\ 10^{-3}$	$1\ 10^{-4}$	-	-	$1\ 10^{-3}$	$1\ 10^{-4}$	$1\ 10^{-3}$	-	$5\ 10^{-4}$	-	$5\ 10^{-4}$	-	-	-	-
S_{sp}	$1\ 10^{-9}$	$0.2\ 10^{-9}$	-	-	-	-	-	-	-	-	$0.2\ 10^{-9}$	-	-	-	-

Table 2 : Additional modifications of the parameters.

		C1	C2	C3	C4	Remarks	
mat 1	K	$1\ 10^{-8}$	-	-	-	K	m/sec
	S_{sp}	$1.69\ 10^{-7}$	-	-	-	S_{sp}	Pa^{-1}
mat 2	K	$1\ 10^{-8}$	-	-	-		
	S_{sp}	$4\ 10^{-7}$	-	-	-		
mat 3	K	$2\ 10^{-8}$	-	-	-		
	S_{sp}	$4\ 10^{-7}$	-	-	-		
mat 4	K	$5\ 10^{-9}$	-	-	-		
	S_{sp}	$4\ 10^{-7}$	-	-	-		
mat 5	K	$5\ 10^{-9}$	-	-	-		
	S_{sp}	$4\ 10^{-7}$	-	-	-		
mat 6	K	$3\ 10^{-9}$	-	-	-		
	S_{sp}	$4.11\ 10^{-7}$	-	-	-		
mat 7	K	$1\ 10^{-8}$	-	-	$5\ 10^{-9}$		
	S_{sp}	$4.11\ 10^{-7}$					
mat 8	K	$5\ 10^{-6}$	-	-	-		
	S_{sp}	$0.22\ 10^{-7}$	-	-	-		
mat 9	K	$5\ 10^{-6}$	$1\ 10^{-8}$	-	-		
	S_{sp}	$3.18\ 10^{-7}$	-	-	-		
mat10	K	$2\ 10^{-5}$	-	-	-		
	S_{sp}	$0.22\ 10^{-7}$	-	-	-		
mat11	K	$1\ 10^{-9}$	-	-	-		
	S_{sp}	$0.1\ 10^{-7}$	-	-	-		
mat12	K	$1\ 10^{-4}$	$5\ 10^{-5}$	-	-		
	S_{sp}	$0.2\ 10^{-9}$	-	-	-		
mat13	K	$2\ 10^{-8}$	-	-	-		
	S_{sp}	$3.18\ 10^{-7}$	-	-	-		
mat14	K	$5\ 10^{-4}$	-	$8\ 10^{-4}$	$7.5\ 10^{-4}$		
	S_{sp}	$0.2\ 10^{-9}$	-	-	-		

Table 3 : Computed subsidence values.

Uncoupled and linear model				Coupled and non-linear model (different running)				P=1.3xR	Additional
Column			1st -> 1990	2nd	3rd	4th	1990	-->2000	subsidence
197	2.02		0.55	0.960	1.019	-	1.019	1.033	0.014
167	1.02		1.02	1.470	-	-	1.470	1.507	0.037
209	2.24		1.62	1.754	-	-	1.754	1.779	0.025
223	2.92		2.80	2.683	2.611	-	2.611	2.643	0.032
207	3.13	2.24	1.25	1.623	-	-	1.623	1.687	0.064
160	3.11	2.47	2.17	2.198	-	-	2.198	2.238	0.040
192	2.32		1.67	2.048	-	-	2.048	2.096	0.048
74	1.21		2.33	2.325	-	-	2.325	2.380	0.055
217	1.11		0.52	0.827	0.998	-	0.998	1.033	0.035
185	1.26		1.63	2.278	-	-	2.278	2.311	0.033
181	1.76		1.58	2.259	-	-	2.259	2.303	0.044
150	1.71		2.17	2.280	-	-	2.280	2.319	0.039
156	1.39		1.23	1.542	1.708	1.881	1.881	1.946	0.065
137	2.09		1.97	2.525	-	-	2.525	2.577	0.052
104	0.90		1.40	1.688	1.832	-	1.832	1.877	0.045
70	1.08		1.51	1.982	-	-	1.982	2.031	0.049
36	1.12		0.95	1.492	-	-	1.492	1.519	0.027
15	0.76		1.72	1.718	-	-	1.718	1.761	0.043
13	2.03		1.42	1.563	-	-	1.563	1.602	0.039
6	0.92		0.96	1.207	-	-	1.207	1.235	0.028
127	2.14		2.06	2.032	-	-	2.092	2.125	0.033
135	2.09		2.05	2.085	-	-	2.085	2.124	0.039
144	2.97		1.34	1.807	-	-	1.807	1.855	0.048
212	1.51		1.58	2.281	1.532	1.867	1.867	1.912	0.045
28	1.50		1.29	1.630	-	-	1.630	1.677	0.047
8	1.91		1.05	1.250	-	-	1.250	1.276	0.026
61	1.76		1.23	1.697	-	-	1.697	1.740	0.043
32	2.13		0.82	1.288	1.319	-	1.319	1.345	0.026
108	3.18		3.12	2.948	-	-	2.948	3.027	0.079
101	1.96		1.79	2.187	-	-	2.187	2.250	0.063
57	3.08		1.72	1.602	1.742	-	1.742	1.778	0.036
106	1.89		1.63	1.556	1.549	1.815	1.815	1.849	0.034

As mentioned previously (Dassargues *et al.*), the points where total subsidence was recorded before 1965 are concentrated in a small area. Moreover, the recorded subsidence is due to the compaction of the 300 meters of loose sediments. The part due to the upper 70 m is not known with accuracy. The values indicated on Figure 16 correspond respectively to 60 % and 90 % of the total subsidence. During the calibration procedure of the flow-compaction model it will be verified that the computed subsidence lies within this range.

Out of this zone, the lack of available data has forced us to make a kind of "blind calibration". In the columns where surprising values are found for subsidence and stress values some changes in the parameter values have been made, within the normal range of variations of the geomechanical parameters and taking into account the spatial distribution of the pore water decrease given by the 3D flow model.

Such minor changes in parameters have led to the computed subsidence values given in Table 3, with an evolution in time until 1989.75 given at the Figures 17 to 24.

The following remarks can be made :

— the compaction is stabilised in each column (the final mean value). This is quite logical since the seasonal stresses remain in the elastic domain and the secondary consolidation is not taken into account;

— the seasonal subsidence shows significant variations : from 5 mm to 5 cm. The amplitude of this variation will only depend on the A values in each column;

— the "elastic rebound" is delayed for some columns. This effect is due to the hydrogeological conditions in the concerned zones, where low permeabilities increase the propagation time for a decrease of pressure in the compressible layers;

— often, the "elastic rebound" is as important as the compaction was before. This seems logical since some empirical relations have been discovered and used between the A and C values;

Simulation of the future subsidence

The results of the 3D flow model with pumping = 1.3 * recharge have been discussed above. Under such con-

Table 4 : 12 types of different typical profiles.

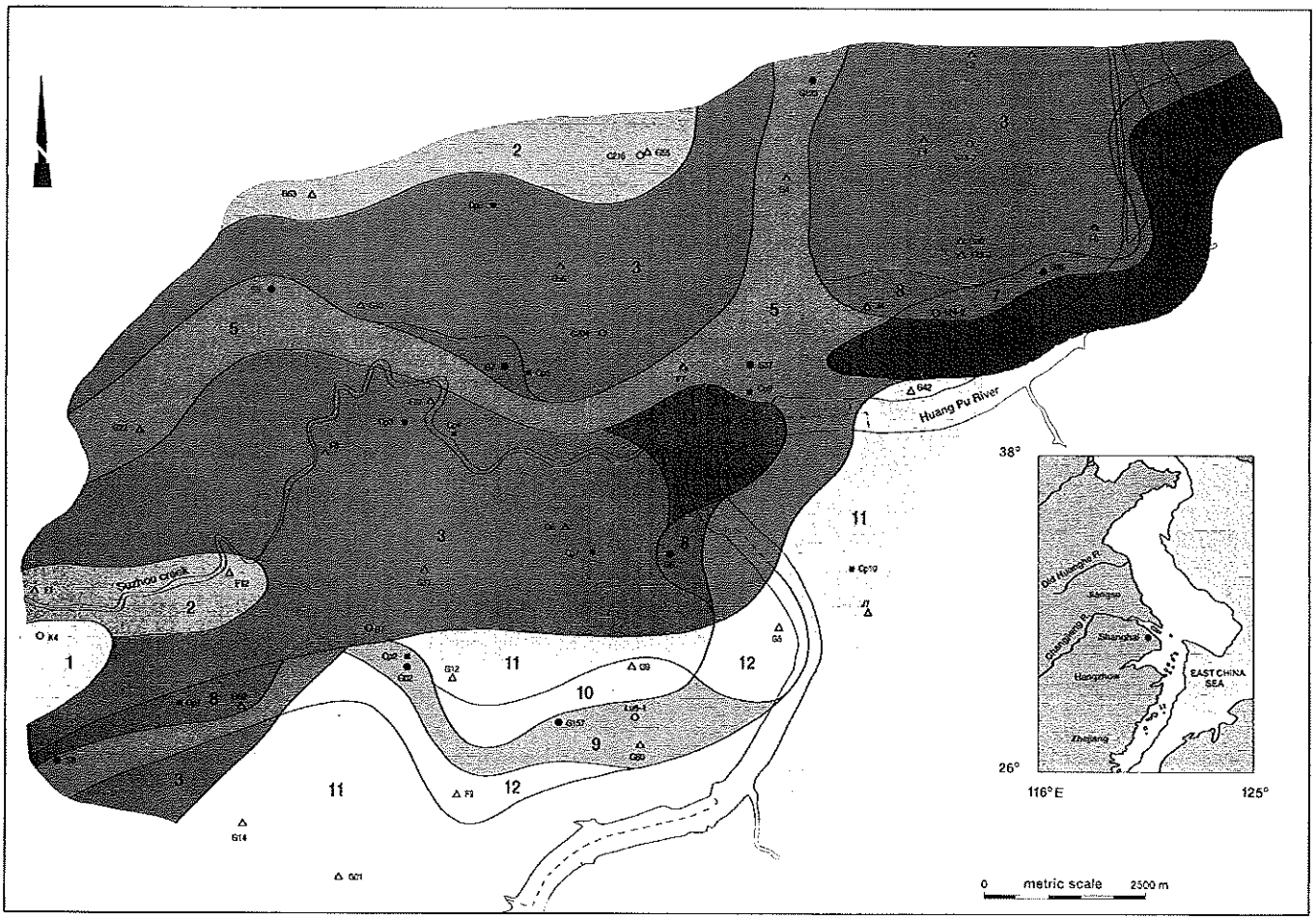

SCHEMATIC SECTION

Explanation of the profile types

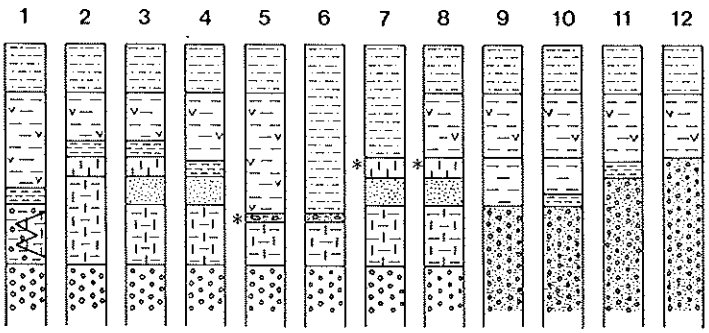

LEGEND OF SCHEMATIC SECTION

Holocene deposits

- 1C - unit
- 2C - unit
- 2Ca - subunit
- Reworked Pleistocene deposits

Upper Pleistocene deposits

- DGSC - unit
- 1A upper - unit
- 1A lower - unit
- 3C - unit
- 3C - unit intercalated with fluvial deposits
- 2A - unit
- Sand complex unit
- * Unit may be absent

ditions and with the same geomechanical parameters, the simulation of the future subsidence until 2000, gives results showing additional subsidence (Fig. 25 to 32). The computed additional compactions are between 1.4 and 7.9 cm as appears on the map (Fig. 33).

Conclusions

The flow model is a full 3D model with a complete discretization of each geological formation in the meshing network. Many values of K and S_s are chosen assuring a very detailed distribution of these hydrodynamic parameters. The 3D flow model gives as results the spatial distribution of the pore pressures as a function of time, the values relative to the clayey layers are not very accurate because of the low permeabilities.

The subsidence computations are completed coupling in the model the vertical flow and the oedometric consolidation processes in the clayey layers.

The pressures computed in the 3D model are introduced in the coupled model as variable prescribed pressures at the aquifer-aquitard boundaries.

The values of A and C have been determined from C_s, C_c and initial void ratio of 1920 (e_i).

The compactions are simulated coupling flow and compaction equations. It supposes that the coefficient of permeability (K) and the specific storage (S_s) can vary with effective stress (σ'). These variations introduce non-linearities in the problem.

The calibration procedure led to modify the discretization and the parameter values, staying in the range of variation determined by the collected data.

Results of the mathematical simulation in "neutral conditions" and in conditions of intensive pumping (pumping = 1.3* recharge) have shown that we can distinguish different zones in the central area of Shanghai, characterized by different sensitivities to land subsidence induced by water withdrawal. These zones can be correlated with the 12 profile types determined by the Quaternary geology study (Table 4).

The less sensitive zones seem to correspond to the profile types 9, 10, 11 and 12 where the *1st and 2nd aquifer* have interconnections and the *3rd compressible layer* is absent.

The more sensitive zones correspond to the profile type 5 where the *DGSC layer* is absent and the thickness of the *1st, 2nd* and *3rd* compressible layers is maximum.

However, an important remark is to formulate about the lateral flow conditions and the way to take them into account in the model. To study more accurately the groundwater resources of the zone it would be necessary to have more information and data about the hydrogeological parameters and subtractions and additions (pumping/recharge) in a large zone surrounding the studied one.